Universidade de Lisboa

Faculdade de Medicina de Lisboa

Impact of NLRP3 Inflammasome Inhibition on a Model of Aβ-Induced Toxicity

Diogo André Mendonça Dias

Orientadora:

Doutora Cláudia Alexandra dos Santos Valente de Castro

Dissertação especialmente elaborada para obtenção do grau de Mestre em Neurociências

2021

Universidade de Lisboa

Faculdade de Medicina de Lisboa

Impact of NLRP3 Inflammasome Inhibition on a Model of Aβ-Induced Toxicity

Diogo André Mendonça Dias

Orientadora:

Doutora Cláudia Alexandra dos Santos Valente de Castro

Dissertação especialmente elaborada para obtenção do grau de Mestre em Neurociências

2021

“A impressão desta dissertação foi aprovada pelo conselho Científico da Faculdade de Medicina de Lisboa em reunião de 19 de janeiro de 2021.”

Acknowledgements

Já dizia Platão que ‘A maior vitória é conquistar a si mesmo’. De facto, a elaboração de um projeto ambicioso, como uma dissertação de mestrado, é um processo longo e acidentado que requer resiliência para superar as numerosas imprevisibilidades que surgem no seu desenvolvimento. No entanto, são desafios como este, dos quais somos principais pensadores e executores, que nos proporcionam a aquisição de competências necessárias para suportar a exigência de um mundo profissional competitivo e em constante atualização.

É da maior importância salientar o papel daqueles que sempre me apoiaram e acompanharam todas as etapas deste desafio. Nomeadamente, agradeço à minha orientadora, ***Professora Cláudia Valente***, pelas suas competências e trajeto inspiradores, o seu suporte permanente e opiniões construtivas. Fico grato pela confiança e pelo sentido de responsabilidade que me incutiu em todas as fases do trabalho.

À ***Professora Ana Sebastião*** agradeço a oportunidade de integrar o seu grupo de investigação, a liderança exemplar do mesmo e a partilha de conhecimentos.

A todos os meus colegas de laboratório quero agradecer pela partilha de experiências e auxílio prestado em diversos momentos. Um agradecimento especial aos membros do meu grupo, os ‘Valentes’, nomeadamente ao ***Francisco Meda***, à ***Mafalda Carvalho*** e à ***Mariana Van-Zeller***, a quem fico grato pelo companheirismo, entreajuda, partilha e respeito.

Por fim, agradeço aos meus amigos de longa data, aos meus irmãos, à minha namorada, aos meus pais e aos meus avós, por acreditarem em mim, por me apoiarem incondicionalmente, pela paciência nos momentos de desânimo e pela felicidade nos momentos de conquista. Tudo o que sou e conquistei, a eles se deve e, como tal, a eles dedico este trabalho.

Diogo Dias

Index

List of Figures

List of Tables

List of Abbreviations

aCSF Artificial cerebrospinal fluid

AD Alzheimer's disease

AICD Amyloid precursor protein intracellular domain

ANOVA Analysis of variance

AP-1 Activator protein 1

ApoE Apolipoprotein E

APP Amyloid precursor protein

ASC Apoptosis-associated speck-like protein containing a CARD

ATP Adenosine triphosphate

Aβ Amyloid-β

BACE β-site APP cleaving enzyme

BBB Blood brain barrier

BSA Bovine serum albumine

C3 Complement component 3

CA Capture antibody

CA Cornu ammonis

CARD Caspase-activation and recruitment domain

CD68 Cluster of differentiation 68

cLB Complete lysis buffer

CNS Central nervous system

CTE Chronic traumatic encephalopathy

CTL Control

DA Detection antibody

DAMP Damage associated molecular pattern

DG Dentate gyrus

DGAV Direção Geral de Alimentação e Veterinária

DNA Deoxyribonucleic acid

ELISA Enzyme Linked ImmunonoSorbent Assay

EOAD Early onset Alzheimer's disease

GABA Gamma-aminobutyric acid

GAPDH Glyceraldehyde-3-phosphate dehydrogenase

GFAP Glial fibrillary acidic protein

GSDMD Gasdermin D

GSDMD-CT Gasdermin D C-terminal

GSDMD-NT Gasdermin D N-terminal

HMGB1 High mobility group box 1

HRP Horseradish peroxidase

Iba-1 Ionized calcium-binding adaptor molecule 1

IF Fluorescence-coupled immunohistochemistry

IFN-ϒ Gamma interferon

IHC Immunohistochemistry

IL Interleukine

IMM Instituto de Medicina Molecular

LOAD Late onset Alzheimer's disease

LPS Lipopolysaccharides

LRR Leucine rich repeat domain

LSCM Laser scanning confocal microscopy

LTP Long-term potentiation

MAPK Mitogen-activated protein kinase

MRI Magnetic resonance imaging

MWM Molecular weight marker

NADPH Nicotinamide-adenine dinucleotide phosphate

NEK NIMA-related kinases

NeuN Neuronal nuclei marker

NF-κB Nuclear factor kappa-light-chain-enhancer of activated B cells

NIMA Never in mitosis gene A

NLR Nod-like receptor

NLRP3 NLR family pyrin domain containing 3

NMDA N-methyl-D-aspartate

NO Nitric oxide

NOD Nucleotide-binding oligomerization domain

NOX NADPH oxidase

ORBEA Órgão Responsável pelo Bem-Estar Animal

PAGE Polyacrylamide gel electrophoresis

PAMP Pathogen associated molecular pattern

PBS Phosphate-buffered saline

PFA Paraformaldehyde

PMSF Phenylmethylsulfonyl fluoride

Pro-IL-1β Interleukine-1β precursor protein

PRR Pattern-recognition receptor

PTM Photomultiplier

PVDF Polyvinylidene fluoride

PYD Pyrin domain

RAGE Receptor for advanced glycation endproducts

RD Reagent diluent

RNS Reactive nitrogen species

ROS Reactive oxygen species

RT Room temperature

SDS Sodium dodecyl sulphate

SEM Standard error of the mean

SNP Single-nucleotide polymorphism

TACE TNFα-converting enzyme

TBI Traumatic brain injury

TBS Tris-buffered saline

TBST Tris-buffered saline with Tween-20

TLR Toll-like receptor

TNFα Tumor necrosis factor alpha

TREM2 Triggering receptor expressed on myeloid cells 2

USA United States of America

WB Washing buffer

WB Western Blot

Abstract

Alzheimer's disease (AD) is a chronic and progressive neurodegenerative disease, considered the most common cause of dementia in the elderly population. Its rapid progression makes the quality of life of patients and their relatives/caregivers devastating. In addition, AD economic impact is very significant, as trillions of dollars are spent each year in disease care.

Since its discovery in 1907, AD has been intensively studied, but no cure or effective preventive strategy has yet been discovered. At the cellular level this pathology is characterized by loss of synapses, neuronal death, intracellular neurofibrillary aggregates of Tau phosphorylated protein and extracellular peptide β amyloid (Aβ) deposition. However, several aspects of this disease are still unknown, such as the mechanisms of neuronal death induced by Aβ.

Recently AD has been associated with inflammatory events, in particular the activation of a multiprotein cytoplasmic complex, NLRP3 inflammasome. This complex is involved in the activation of Caspase-1 and subsequent production of pro-inflammatory cytokines such as Interleukine-1β (IL-1β) and IL-18, and cleavage of Gasdermin D (GSDMD), associated with pyroptosis, a type of inflammatory cell death.

Several studies have suggested a diarylsulfonylurea-containing small molecule, named MCC950, as a potent and selective NLRP3 oligomerization inhibitor, that does not affect the role of other inflammasomes, hence avoiding immunosuppressive effects.

This project has three main objectives: 1) to establish a model of Aβ-induced toxicity in acute slices, 2) to characterize the Aβ-induced neuroinflammatory milieu in this system, and 3) to evaluate the potential protective effect of MCC950 upon Aβ impact. The work was performed in acute slices of hippocampus extracted from 7 to 8 weeks old Wistar rats, which were subsequently exposed to $A\beta_{1-42}$ oligomers. Western Blot assays and Enzyme Linked Immunosorbent Assay were used to evaluate glial activation, and inflammasome priming and oligomerization. Afterwards, the effect of NLRP3 inflammasome inhibitor

MCC950 was addressed, to check whether it was capable or not to prevent the $A\beta_{1-42}$-induced noxious effects.

Indeed, our results show that $A\beta_{1-42}$ oligomers triggered the reactive phenotypes of astrocytes and microglia, in a process known as reactive gliosis, and induced inflammasome priming and activation, causing increased expression of Caspase-1 and Caspase-1-mediated processing of IL-1β, as well as the expression of the cleaved form of GSDMD, known to oligomerise in the inner side of the cell membrane, creating pores typical of cellular death by pyroptosis. On the other hand, MCC950 prevented inflammasome priming and activation and its respective correlates, namely, it decreased reactive gliosis and the expression of inflammasome-driven events, as production of active Caspase-1 and cleaved GSDMD. However, as MCC950 does not affect the inflammasome priming step, it did not influence the $A\beta_{1-42}$-induced increased expression of NLRP3 protein and IL-1β. Their expression continues increased in the presence of MCC950 due to the induction of the NF-κB pathway by the $A\beta_{1-42}$ oligomers.

Overall results show that $A\beta_{1-42}$ oligomers induce a powerful neuroinflammatory context in acute hippocampal slices, mediated by NLRP3 inflammasome, and reinforce the hypothesis that $A\beta_{1-42}$ toxic species eventually lead to cellular death by pyroptosis. Moreover, this work highlighted the role of MCC950 as an effective NLRP3 inflammasome inhibitor, further strengthening its potential as a drug for AD.

Keywords: Alzheimer's disease, Aβ, NLRP3 Inflammasome, Gliosis, Pyroptosis, MCC950

Resumo

A doença de Alzheimer (Alzheimer's Disease - AD) é uma doença neurodegenerativa crónica e progressiva, considerada a causa mais comum de demência na população idosa. A sua rápida progressão torna devastadora a qualidade de vida dos doentes e dos seus parentes/cuidadores. Além disso, o impacto económico da AD é muito significativo, uma vez que triliões de dólares são gastos todos os anos no tratamento da doença. Atualmente, a ideia de um fármaco único para AD é considerada utópica. À medida que o conhecimento sobre a doença aumenta, mais investigadores se apercebem de que esta é de facto consequência de uma complexa cascata de eventos com muitas redes de interações. Por esta razão, é mais provável que um tratamento futuro possa surgir de combinações de diferentes fármacos que visem pontos de controlo cruciais no desenvolvimento da doença.

Desde a sua descoberta em 1907, a doença tem sido intensamente estudada, embora ainda não tenha sido descoberta nenhuma cura ou estratégia eficaz de prevenção. A nível celular, esta patologia é caracterizada pela perda de sinapses, morte neuronal, agregados neurofibrilares intracelulares de proteína Tau fosforilada e deposição extracelular do péptido β amilóide (Aβ). No entanto, vários aspetos desta doença são ainda desconhecidos, tais como os mecanismos de morte neuronal induzida por Aβ.

Este trabalho baseia-se na hipótese da cascata amilóide, que considerando dados genéticos e histopatológicos, sugere que depósitos tóxicos de Aβ no cérebro desencadeia uma sequência de eventos que culminam na ativação crónica das células gliais (gliose) criando um ambiente neuroinflamatório, danificando progressivamente os neurónios, alterando a homeostase iónica, aumentando o stress oxidativo e causando eventualmente a morte generalizada das células.

O hipocampo é surpreendentemente suscetível a insultos, sendo uma das áreas do cérebro mais afetadas por patologias relacionadas com o envelhecimento, como a AD. De facto, várias evidências sugerem que é a primeira região do cérebro a apresentar sinais de neurodegeneração, bem como consequentes alterações estruturais, especialmente perda de volume.

Recentemente, a AD tem sido associada a eventos inflamatórios, especificamente a inflamassomas, complexos multiproteicos citosólicos que medeiam respostas imunes. Vários inflamassomas foram descritos, no entanto, o inflamassoma NLRP3 é o mais intensivamente estudado, sendo a sua ativação reconhecida como um componente central no desenvolvimento de várias doenças inflamatórias e autoimunes. Foi observada uma ativação exacerbada da via do NLRP3 nas doenças cerebrais e alguns estudos sugerem que este inflamassoma desempenha um papel fundamental na disfunção comportamental e cognitiva observada na AD, pelo que a sua inibição pode resultar em efeitos terapêuticos e/ou preventivos significativos. Este complexo está envolvido na ativação da Caspase-1 e subsequente produção de citocinas pró-inflamatórias como a Interleucina-1β (IL-1β) e a IL-18, e processamento da Gasdermin-D (GSDMD), associada à morte celular por piroptose.

A piroptose é um tipo de morte celular programada, dependente da ativação de caspases inflamatórias, tais como a Caspase-1. Estudos recentes mostraram que a piroptose está associada a uma variedade de doenças neurodegenerativas devido ao seu efeito pró-inflamatório e disfunções celulares relacionadas. Morfologicamente, a piroptose é caracterizada pela formação de poros na membrana plasmática, levando à libertação de citocinas inflamatórias e outros sinais de stress celular, perpetuando assim o efeito inflamatório. A Caspase-1 promove a clivagem da proteína GSDMD, formando-se o fragmento N-terminal (GSDMD-NT), que é subsequentemente translocado para o interior da membrana plasmática, onde se conecta aos fosfatos fosfatidilinositol e fosfatidilserina, oligomerizando e originando poros.

As células gliais consistem em macroglia, tais como astrócitos e oligodendrócitos, e microglia. Destas, as microglias são consideradas os macrófagos do cérebro, embora atualmente se saiba que os astrócitos também têm um papel crucial nas respostas imunitárias do sistema nervoso central. As células gliais possuem recetores de reconhecimento de padrões, como NLRP3, capazes de detetar sinais de stress ou derivados de patógenos.

Existem duas principais vias de ativação do inflamassoma NLRP3: a via canónica e a via não canónica. A primeira, sobre a qual este trabalho incide, requer um sinal de priming e um sinal de ativação ou oligomerização. Nos últimos

anos, vários estudos têm enaltecido o potencial de um composto, MCC950, considerado um potente e seletivo inibidor de oligomerização do inflamassoma NLRP3, que não afeta o papel de outros inflamassomas, como o NLRP1, evitando assim efeitos imunossupressores.

Este projeto tem três objetivos principais: 1) estabelecer um modelo de toxicidade induzida por Aβ em fatias agudas de hipocampo, 2) caracterizar o meio neuroinflamatório induzido por Aβ, e 3) avaliar o potencial efeito protetor do MCC950 sobre o impacto de Aβ. O estudo foi realizado em fatias agudas de hipocampo obtidas de ratos Wistar com idades compreendidas entre 7 a 8 semanas, que foram subsequentemente expostas a oligómeros de $A\beta_{1-42}$. Os ensaios de Western Blot (WB) e de Enzyme Linked Immunosorbent Assay (ELISA) foram utilizados para avaliar a ativação glial, as etapas de priming e oligomerização do inflamassoma, e a ocorrência de morte por piroptose. Posteriormente, foram avaliados os efeitos do inibidor do inflamassoma NLRP3, MCC950, para verificar a sua capacidade de contrariar os efeitos nocivos induzidos por $A\beta_{1-42}$.

Os nossos resultados indicam que $A\beta_{1-42}$ induziu o priming e a ativação do inflamassoma NLRP3, desencadeando consequentemente o fenótipo reativo de astrócitos e microglia, num processo conhecido como gliose, e aumentando a produção de IL-1β, bem como a expressão da forma clivada de GSDMD, conhecida por migrar para o lado interno da membrana celular, criando poros e conduzindo a morte celular por piroptose.

Por sua vez, o inibidor seletivo do inflamassoma NLRP3, MCC950, impediu a ativação do inflamassoma e o seu impacto, diminuindo a gliose, e a expressão da Caspase-1 ativa e da GSDMD clivada. Contudo, uma vez que o MCC950 não afeta a etapa de priming do inflamassoma, as expressões das proteínas NLRP3 e IL-1β não foram influenciadas, continuando aumentadas na presença do inibidor devido à ativação da via NF-κB pelos oligómeros de $A\beta_{1-42}$. Os níveis de Caspase-1 e GSDMD-NT foram reestabelecidos na presença de MCC950, confirmando que o inibidor impediu a oligomerização do inflamassoma, afetando a conversão da pro-Caspase-1 em Caspase-1 ativa, e consequentemente a clivagem da GSDMD. Finalmente, os níveis do domínio ASC, inalterados pelos oligómeros de $A\beta_{1-42}$, não sofreram alterações na presença do MCC950.

Com a oligomerização do inflamassoma impossibilitada, o processamento e libertação de citocinas pró-inflamatórias ficaram comprometidos. Por esta razão, na presença do MCC950 é inibida a ativação da via NF-κB em astrócitos e prevenida a conversão para o fenótipo neurotóxico A1. O MCC950 não só impediu a ocorrência de astrogliose, como também a ativação da microglia. Os resultados revelaram que o MCC950 conduziu à diminuição significativa da expressão do marcador de microglia reativa CD68, induzida pelos oligómeros de $A\beta_{1-42}$.

Sumariamente, os resultados deste trabalho demonstram que $A\beta_{1-42}$ induz uma poderosa resposta neuroinflamatória, mediada pelo inflammasoma NLRP3, e reforçam a hipótese de que os oligómeros tóxicos de Aβ originam a morte celular por piroptose. Além disso, foi realçado o papel do MCC950 como um inibidor eficaz do inflamassoma NLRP3, capaz de impedir os efeitos da sua ativação e reforçando assim o seu potencial terapêutico.

Avanços científicos recentes relativos ao desenvolvimento de técnicas não invasivas para a deteção *in vivo* de depósitos de Aβ, permitem que a doença seja detetada antes de esta se começar a manifestar. Neste contexto, a administração preventiva de MCC950 poderá ser decisiva para impedir a perda celular causada por processos inflamatórios nocivos, evitando, consequentemente, o aparecimento de sintomas.

À medida que o conhecimento sobre a doença aumenta, mais claro é o facto de que AD é resulta de uma complexa cascata de eventos com muitas redes de interações. Por esta razão, é provável que uma abordagem farmacológica futura surja da combinação de diferentes medicamentos que visem pontos de controlo cruciais para o desenvolvimento da doença.

Palavras-chave: Doença de Alzheimer, Aβ, Inflamassoma NLRP3, Gliose Piroptose, MCC950

‘Nothing in life is to be feared, it is only to be understood.

Now is the time to understand more, so that we may fear less.’

Marie Currie[1]

1. Introduction

1.1. Alzheimer's disease

Alzheimer's disease (AD) is the most common type of dementia among elderly population, affecting 50 million people worldwide and accounting for 50-70% of all cases of dementia, according to the World Health Organization. AD is currently incurable, and its recurrence is likely to increase due to population ageing. It is a chronic pathology with around two decades of preclinical and prodromal phases, in which the pathology develops silently, and an average clinical duration of 8–10 years, characterized by progressive memory loss and cognitive decline[2,3]. Eventually, at later stages, patients start struggling with motor functions such as speaking, walking and swallowing[2].

Regarding the prevalence, estimates indicate 10–30% of the population over 65 years of age with an incidence of 1–3%[3]. The majority of AD patients (>90%) have the late onset AD or LOAD (80–90 years of age)[4], sporadic form, caused by the inability to clear the amyloid-β (Aβ) peptide from the brain[3]. Less than 1% have inherited mutations in genes that affect processing of Aβ and develop the disease at a younger age (mean of ~45 years). In these cases, the disease is called an early onset AD or EOAD[3].

This work is based upon the undisputed amyloid cascade hypothesis[5], which considering genetic and histopathological data, suggests that toxic deposits of Aβ in the brain trigger a sequence of events that culminate in the AD dementia, namely, chronic activation of glial cells (gliosis) that create a neuroinflammatory environment, progressively injuring neurons, altering ionic homeostasis, increasing oxidative stress and eventually causing generalised cell death[6].

In conclusion, AD is a multifactorial disease that represents a major public health concern, not only causing great suffering to patients, relatives and/or caregivers, but also resulting in a great economic burden to society. It is estimated that the costs related with the disease will increase up to 2 trillion dollars in 2030[7-9]. In this context, the main challenges for science and medicine are to be able to address the weaknesses of the amyloid cascade hypothesis by

achieving a more complete mapping of all processes and interactions that lead to the disease, the lack of reliable biomarkers for its early diagnosis as well as the lack of preventive strategies and effective treatments[10,11].

1.1.1. Neuropathology

AD is classically characterised by four pathological hallmarks, these being the presence of extracellular Aβ plaques and intracellular hyperphosphorylated tau tangles, firstly described by Alois Alzheimer in 1907[12], the increased neuroinflammation, and finally, brain atrophy[4]. The gradual loss of neuronal function and death of neurons leads to an atrophy of the brain which can be observed in post-mortem parenchyma samples[3,12]. Anatomically, AD starts by affecting regions of the brain related with memory and cognition, namely, tissue from limbic system, frontal and temporal lobes, eventually spreading to all regions of the brain (**Fig. 1**)[3,13].

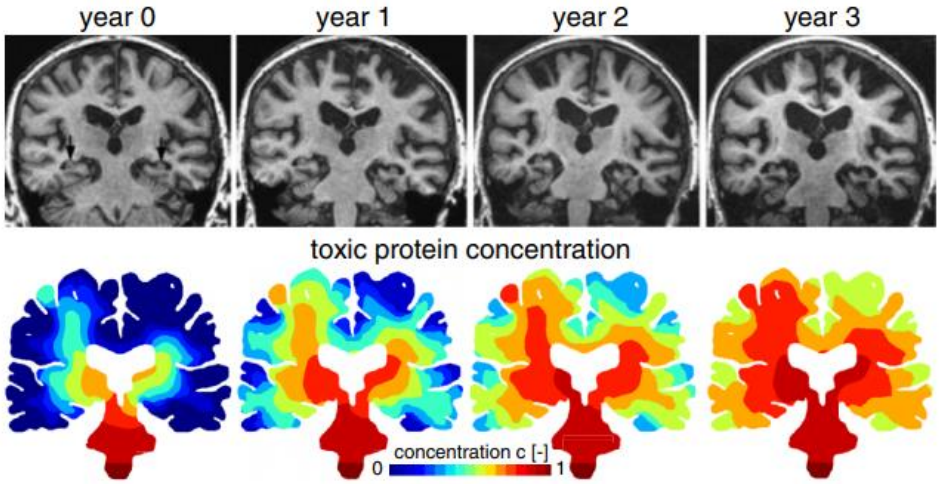

Figure 1. Evolution of Alzheimer's Disease. This figure shows a direct relation between progressive brain atrophy (top row), seen through Magnetic Resonance images, and respective increase and spread of toxic proteins, predicted through a propagation model (bottom row). As a result of the high toxic protein concentrations, it is often observed an unequivocal ventricular enlargement, widening of the cortical sulci and hippocampal atrophy *(Figure adapted from Weickenmeier et al., 2018)*[13].

Aβ is the product of sequential processing of an amyloid precursor protein (APP) by two aspartyl proteases (β- and ϒ-secretases), in a process known as the amyloidogenic pathway (**Fig. 2**)[4,14,15]. Under normal physiological conditions,

the clearance of this peptide is efficient and works either by locally degrading Aβ peptides or by transferring them into cerebrospinal fluid and blood vessels[16]. However, under pathological conditions this clearance becomes inefficient, increasing the vulnerability to the formation of toxic structures which ultimately cause fatal imbalances to the cellular environment[17]. In this context, an abnormal cleavage of APP can originate peptides that contain an unstable high β-sheet structure that makes them prone to oligomerization or aggregation[3]. Also, the most amyloidogenic isoform of Aβ, and the most toxic[4], is the 42 amino-acid isoform ($A\beta_{1-42}$)[18,19]. Overall, the pathological accumulation of Aβ is thought to be a result of reduced clearance and/or increased cleavage of APP through the amyloidogenic pathway.

In addition to toxic protein aggregates, activated astrocytes and microglia, as well as elevated proinflammatory markers, are included in the neuroinflammatory hallmark of all tauopathies[20]. A study showed that small Aβ oligomers and protofibrils are phagocytosed by microglia and can activate all important components of the NLRP3 inflammasome, with Apoptosis-associated speck-like protein containing a CARD (ASC) formation and interleukine-1β (IL-1β) release. The authors suggested that the early neuroinflammatory event can trigger further neuropathological changes and enhance progression or acceleration to AD-associated dementia[18].

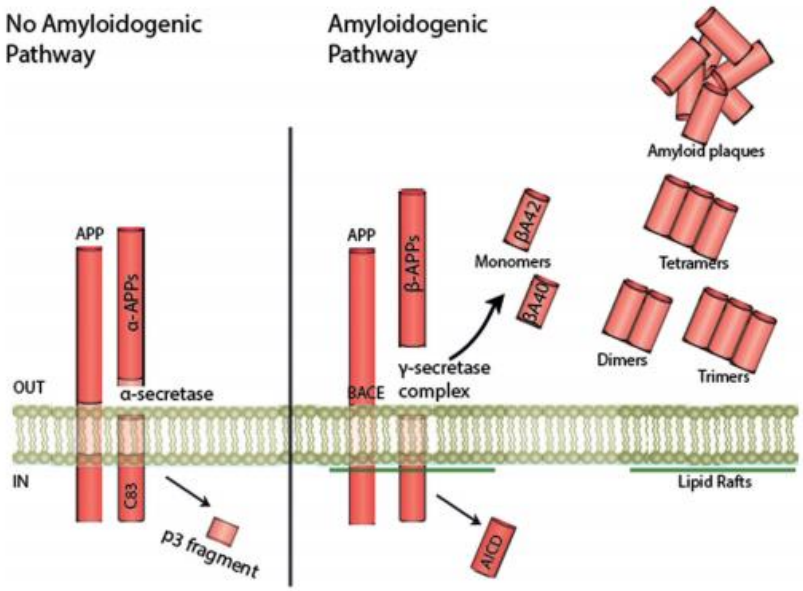

Figure 2. Formation of Aβ. APP is a type I transmembrane protein that suffers two pathways of enzymatic processing. In the non-amyloidogenic pathway α-secretases

(TNFα-converting enzyme - TACE) cleave APP in the Aβ domain, producing a long soluble extracellular domain and a C83 peptide which is cleaved by Ɣ-secretases, originating a p3 fragment that prevents Aβ formation. On the contrary, in the amyloidogenic pathway, β secretases (BACE) cleave the amino terminal of APP, originating a C99 fragment and soluble extracellular peptides of APP (β-APPs), shorter than the ones created by α-secretases in the non-amyloidogenic pathway. The C99 fragment is then cleaved by Ɣ-secretase complexes producing an intracellular domain (AICD), a short peptide $A\beta_{40}$ or a long peptide $A\beta_{42}$, the latter being the most fibrillogenic and neurotoxic specie. It is worth noticing that this pathway, as well as $A\beta_{42}$-induced damage have been strongly associated with areas of the membrane containing lipid rafts *(Figure adapted from Zimbrón et al., 2014)*[15].

1.1.1.2 The Hippocampus in AD

Structurally resembling a seahorse, the hippocampus is a structure of the limbic system positioned in the medial temporal lobe of the cerebral cortex[21]. Crucial in the fields of neuroscience, it is thought to be at the centre of the brain's network, being of upmost importance for the formation, consolidation and retrieval of memories, and also known to regulate emotions, stress and anxiety[21].

This structure is a complex of different substructures, perfectly arranged, these being the dentate gyrus (DG), cornu ammonis 1 (CA1), CA2, CA3, the subiculum, presubiculum, parasubiculum and enthorhinal cortex (EC) . The hippocampal network involves different types of neurons and is mainly uni-directional and dependent on glutamate (**Fig. 3**)[22]. Interestingly, the basic hippocampal architecture is nearly the same in all mammals[23], which makes animal models such as rats, which are genetically, physiologically and morphologically closer to humans than mice, excellent for mimicry procedures and allowing correlation to human contexts[24].

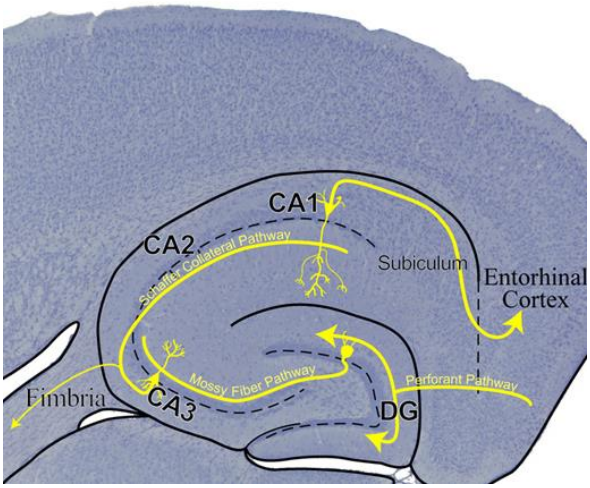

Figure 3. Hippocampal circuitry. This figure shows a horizontal section of the cortex and hippocampus of a rat, where the hippocampal circuitry can be observed. The main inputs occur from the lower layers of EC to the DG, through the Perforant Pathway, subsequently to the CA3, using the Mossy Fiber Pathway, and then to CA1 through Shaffer Collaterals, where they are directed to the subiculum that finally outputs the signal back into the higher layers of EC. *(Figure adapted from Smith et al., 2012)*[22]

The hippocampus is surprisingly susceptible to insults, being one of the brain areas most affected by ageing related pathologies such as AD. In fact, growing evidence suggest that it is actually the first region of the brain to present neurodegeneration signs as well as consequent structural alterations, especially volume loss, which can be detected through Magnetic Resonance Imaging (MRI)[21]. Scientists have developed drugs as cholinesterase inhibitors, to help stabilize or even improve the memories of patients suffering from AD. However, until today all developed drugs are only able to delay or improve the quality of life of the patients, and no drug was yet able to halt the disease.

The role of inflammation in AD has been growing in the past few years, with discovery of novel mechanisms that impact the disease. This topic will be discussed in detail in the next sections.

1.1.2. Neuroinflammation

Neuroinflammation is the inflammation of the nervous tissue (brain and spinal cord) that can be initiated in response to a variety of signs, including infection, traumatic brain injury, toxic metabolites, or autoimmunity. Under normal/ acute physiological conditions its role is to fix and prevent harmful events, however, under pathological conditions, such as AD, it can become uncontrolled, perpetuating itself, thus becoming a chronical inflammation that promotes further damage to the nervous tissue[16,25]. Indeed, Aβ complexes are known to trigger a chronic inflammatory response that causes continuous cell death and neuronal dysfunction[26].

A neuroinflammatory process is always starred by multiprotein cytosolic complexes called inflammasomes, that mediate the immune response. As soon as these structures are assembled, they recognise stress signals, either pathogen-associated molecular patterns (PAMPs), such as lipopolysaccharides (LPS), or damage-associated molecular patterns (DAMPs), such as Aβ, activate caspases which then cleave pro-inflammatory cytokines into their active form[27]. Released pro-inflammatory cytokines and binding to their respective receptors, present on microglia, astrocytes, neurons and endothelial cells, will then initiate a cascade of signalling events that will further perpetuate inflammation.

Activation of glial cells, known as reactive gliosis, and elevated levels of pro-inflammatory mediators are pathological markers present in the brain of AD patients. Recently, scientists have been trying to understand the role of gliosis and neuroinflammation in neurodegenerative diseases, including AD, since increasing evidence suggests that neuroinflammation can be a trigger for these pathologies[26,28].

Genetic studies have implicated roles for the innate immune system in neurodegenerative diseases, particularly AD. Whole exome sequencing studies identified several gene variants that influence the risk of developing AD. An example are the variants of triggering receptor expressed on myeloid cells 2 (TREM2), an immunoglobulin-like cell-surface receptor primarily expressed on microglia in the brain, able to confer a 2 to 4-fold increased risk for the disease[29]. However, the greatest risk factor for late-onset sporadic AD is apolipoprotein E

(ApoE), a peptide mainly secreted by glial cells that functions as a major transporter of lipoproteins between cells in the brain. Specifically, ApoEε4 allele is known to decrease Aβ turnover and clearance, and also to influence directly Aβ aggregation[30,31]. In addition, it is associated with a 4 to 12-fold increased risk based on allele dosage[32]. The exact contributions of TREM2 and ApoE on tau pathogenesis remains unclear and should be more thoroughly assessed in future research.

Environmental factors that promote neuroinflammation, such as toxins and viral infections, can also contribute to the development of the pathogenesis. It is known that traumatic brain injury (TBI) predisposes individuals to AD. Evidence indicate that repetitive mild TBI, can have long-term consequences resulting in tauopathy and neurodegeneration as seen in chronic traumatic encephalopathy (CTE)[33]. Inflammatory impact was shown to persist up to 17 years post-injury, instigating reactive gliosis and prime microglia to over-react to future insults[34]. While acute gliosis is arguably considered protective following TBI, it is hypothesized that repetitive insults provoke microglia and astrocytes to release higher levels of proinflammatory molecules that affect neuronal homeostasis and influence tau release and aggregation[35].

1.1.2.1. NLRP3 Inflammasome

As previously mentioned, inflammasomes play key roles in neuroinflammatory responses. These multiprotein complexes are cytosolic pattern recognition receptors (PRR), and mediate immune responses through the activation of a pro-inflammatory caspase, which then cleaves pro-inflammatory cytokines into their biologically active form[27,36].

Several inflammasomes have been described, however, the NLRP3 inflammasome is the best studied one and its activation is recognized as a central component in the development of several inflammatory and autoimmune diseases[37]. An exacerbated activation of NLRP3 pathway was observed in brain diseases and some studies suggest that this inflammasome plays a key role in behavioural and cognitive dysfunction observed in AD, so its inhibition may result in significant therapeutic and/or preventive effects[37-40].

NLRP3 inflammasome, which stands for NLR family pyrin domain containing 3, is subcategorised within the NLRP family and contains a sensor with three “sub” domains: 1) a leucine rich repeat domain (LRR) at the C-terminal, which has self-regulatory functions and is involved in ligand interaction; 2) a nucleotide binding and oligomerization domain, NOD or NACHT, which has ATPase activity and is essential for the formation of oligomeric structures necessary for the whole assembling of the inflammasome, and 3) a pyrin domain (PYD) at the N-terminal whose function is to mediate the downstream signal transduction. In the centre of the complex lies the adapter protein ASC, which is crucial for the functional assembling of the inflammasome and contains two “sub” domains: an N-terminal PYD domain that binds to the above-mentioned N-terminal PYD domain of NLRP3 through homotypic interactions, resulting in a dimeric assembly; and a C-terminal caspase activation and recruitment domain (CARD) which will interact with the equivalent CARD domain of pro-Caspase-1[36,41,42]. Inactive pro-Caspase-1 is converted to an active enzyme via dimerization, followed by an autocatalytic reaction that generates active Caspase-1, the enzyme responsible for processing pro-inflammatory cytokines, pro-IL-1β and pro-IL-18 [36,41,43].

Also, it is known that other inflammasomes, such as NLRP10, can link to ASC, thus impeding the assembly of NLRP3 inflammasome. However, a study showed that as aggregated $A\beta_{1-42}$ is phagocytized, cathepsins are eventually released and subsequently degrade NLRP10 inflammasome, allowing ASC to assembly with the NLRP3 domain[44].

There are other proteins whose importance for inflammasome activation have been increasingly highlighted by researchers. The best characterized is a protein of the Never in Mitosis gene A (NIMA)-related kinases (NEK) family in mammals, which interacts with the LRR domain of NLRP3 inflammasome, acting downstream of the K^+ efflux, thus regulating the oligomerization and activation of NLRP3 inflammasome. It is also postulated that K^+ efflux induces conformational changes in the inflammasome, enabling the binding of NEK7[36,45,46]. Finally, Dopamine can act as an endogenous inhibitor of NLRP3 inflammasome activation[47].

1.1.2.2. Activation of NLRP3 Inflammasome

There are two major forms of activation of the NLRP3 inflammasome: the canonical pathway and the non-canonical pathway. The first one requires a priming and an activation signal (**Fig. 4**).

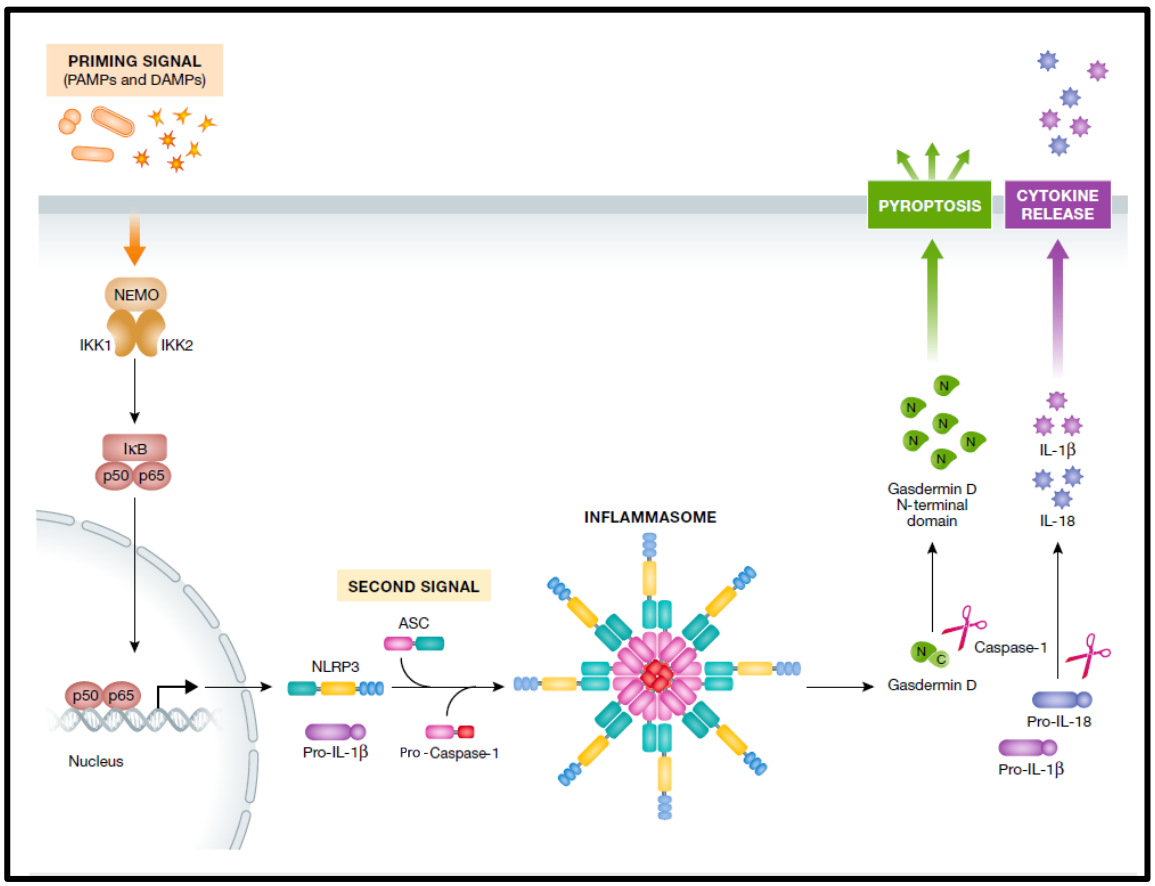

Figure 4. Canonical pathway of NLRP3 inflammasome activation and consequent cytokine release and cell death by pyroptosis. Activation of the NLRP3 inflammasome involves a two-step mechanism. The priming signal by PAMPs and DAMPs, detected by membrane-bound PRRs, induce NF-κB-dependent transcription of NLRP3 and pro-IL-1β precursor protein, and controls post-translational modifications that license NLRP3 activation. Then, a second activation signal is required for inflammasome assembly, causing the oligomerization of NLRP3 sensor protein, adapter protein ASC and pro-Caspase-1. Active Caspase-1 then cleaves pro-IL-1β and pro-IL-18 to their mature forms, IL-1β and IL-18, respectively, which get secreted. Additionally, Caspase-1 can cleave gasdermin D, releasing its N-terminal fragment which translocates to the plasma membrane inducing pore formation and cell death by pyroptosis. Note that toxic Aβ oligomers are known to induce both priming and activation signals. *(Figure adapted from Voet et al., 2019)*[48]

The priming signal is provided by the nuclear factor kappa-light-chain-enhancer of activated B cells (NF-κB)-activating stimuli which promotes *de novo* synthesis of NLRP3 domain and pro-IL-1β, and controls the post-translational modifications of NLRP3, such as its deubiquitination required for subsequent oligomerization[36,49,50]. Note that physiologically, NF-$_k$B performs important functions such as neurite outgrowth, synaptic plasticity and neuronal survival, all of which are known to be impaired in AD[51]. The priming stimulus can be evoked either by endogenous molecules, such as IL-1β and Aβ, or by exogenous microbial molecules such as toll-like receptor (TLR) ligands[52].

The diverse chemical and structural nature of the NLRP3-activating stimulus suggests that they do not interact with the inflammasome, but instead produce common signals that do so. Thus, studies suggest that the signals are various factors such as decreased intracellular potassium concentration, reactive oxygen species (ROS) and mitochondrial deoxyribonucleic acid (DNA) released from damaged mitochondria, release of cathepsins to cytosol by endo-lysosomal destabilization, calcium-dependent flow and signalling, among others[36,53].

The noncanonical activation route depends mostly on the action of caspase-11 in mouse (Caspase-4 and Caspase-5 in humans), which once activated by Gram-negative bacteria, activates the NLRP3 inflammasome promoting the release of IL-1β and IL-18, also regulating the release of IL-1α and high mobility group box 1 (HMGB1) and promoting cell death[53,54].

1.1.2.3. NLRP3 Inflammasome in AD

Since the mid-90s, when it was first shown that the levels of IL-1β are increased in the cerebrospinal fluid of AD patients[55], researchers have been increasingly exploring the role of inflammation in this disease. Meanwhile, the spotlight was swiftly taken by NLRP3 inflammasome activation in microglia, due to experiments that demonstrated that inflammasome components such as NLRP3 protein and Caspase-1 are significantly increased in the brains of AD patients[38]. The same study also used a mouse model of AD to demonstrate that absence or depletion of either NLRP3 or Caspase-1, mitigates spatial memory deterioration and promotes the elimination of Aβ from the neuronal environment[38].

In the context of canonical activation (**Fig. 4**), Aβ serves as priming stimulus, through binding with the pattern-recognition receptor CD36, which then creates a receptor complex with TLR4-TLR6 heterodimer (CD36/TLR4/TLR6), leading to the translocation of NF-κB to the nucleus, consequently promoting the transcription of the NLRP3 domain of the inflamassome[56]; and also activating stimulus, as after phagocytosis of Aβ, the reactive products that form inside lysosomes, namely thioflavin-reactive amyloid, promote destabilization of the lysosomal environment, causing the activation and release of proteolytic enzymes, such as cathepsin B, that promote the assembly of the inflammasome, through an yet obscure mechanism[56]. Another possible explanation for inflammasome activation is through adenosine triphosphate (ATP) binding to P2X7 purinergic receptors, which promote K^+ efflux[57].

Other studies indicate that higher levels of IL-1β induce tau-hyperphosphorylation, further compromising long-term potentiation (LTP) and consequently affecting synaptic plasticity, learning and memory[58,59]. Also, it was found that genetic variations in the NLRP3 gene, such as single-nucleotide polymorphisms (SNPs), may impact LOAD with synergistic effects[60].

1.1.2.4. MCC950, a Selective Inhibitor of the NLRP3 Inflammasome

Since the discovery of NLRP3 in 2001, many institutions around the world focused their efforts on developing drugs capable of halting the action of NLRP3 inflammasome activation aiming to treat a wide range of diseases where inflammation plays a significant role. In fact, pharmaceutical companies such as Inflazome and Novartis are currently undergoing preclinical or phase I and II clinical trials for their still undisclosed molecules. An example is NodThera's NT-0167 which has shown promising NLRP3 inhibition reducing IL-1β production in preclinical studies and is currently being tested in phase I clinical trials[61].

Indeed, investigations have uncovered various inhibitors of the NLRP3 inflammasome pathway, which were validated through *in vitro* studies and *in vivo* experiments in animal models of NLRP3-associated disorders. Pharmacological inhibitors of NLRP3 inflammasome, either directly or indirectly, were exhaustedly reviewed by Zahid and co-workers[62].

However, the diarylsulfonylurea-containing small molecule, termed as MCC950, is considered a potent and selective NLRP3 inhibitor. MCC950 binds non-covalently to the Walker B motif within the NLRP3 domain, thereby blocking the ability of NLRP3 to hydrolyse ATP, inhibiting NLRP3 oligomerization[63] and consequently halting inflammasome activation, either through canonical or non-canonical pathways (**Fig. 5**)[63,64].

Data from the same study also revealed that the molecule does not inhibit neither the TLR signalling nor the priming phase of NLRP3 activation[64]. It was also observed that MCC950 did not change the expression of pro-Caspase-1, pro-IL-1β or ASC, nor did it affect K^+ efflux, Ca^{2+} flux or NLRP3-ASC interactions[64]. MCC950 inhibited the formation of ASC speck resulting from NLRP3 activation, but did not decrease the NLRP1-mediated speck formation, proving the specificity of this molecule towards NLRP3. This conclusion was further strengthened by the fact that the production of IL-1β during *in vivo* infection responses was not impaired, meaning that apart from NLRP3, other inflammasomes pathways were active. Finally, a later study using an *in vivo* APP/PS1 mouse model, showed that MCC950 improves cognitive function as it promoted Aβ phagocytosis[37].

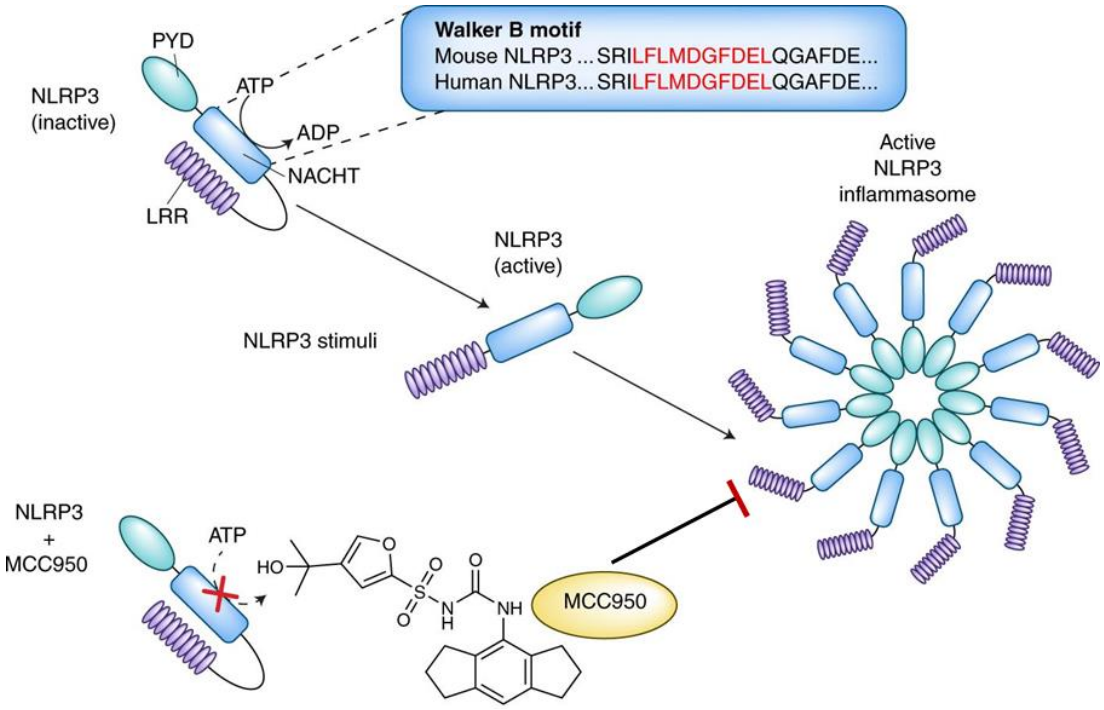

Figure 5. Mechanism of action of MCC950. MCC950 specifically binds to both active and inactive NLRP3, in a high-affinity non-covalent interaction at or adjacent to the Walker B motif. This event blocks the ability of NLRP3 to hydrolyse ATP, consequently impeding the conformational change required for the assembling to occur. (*Figure adapted from Coll et al., 2019*)[63]

1.1.2.5. Glial Cells

The blood brain barrier (BBB) is a semipermeable “filter” that impedes non-selective solute and cells to cross from the blood to the central nervous system (CNS)[65]. Blocking the entrance of pathogens, and allowing the passage of O^2, glucose and hormones, are among the many crucial roles that this structure performs[65]. Thus, the brain is almost immune-isolated from the rest of the body, and it has its own immune cells.

Glial cells consist of macroglia, such as astrocytes and oligodendrocytes, and microglia. Of these, microglia are considered the macrophages of the brain, and astrocytes are nowadays believed to have a crucial role in CNS immune responses[66]. Also, glial cells possess PRRs, either membrane bound, such as TLRs, or cytosolic, like NLRs, capable of sensing stress signals in the form of PAMPs and DAMPs[25,67,68].

Some pathological conditions can disturb the BBB, allowing the entrance in the CNS of cells of the peripheral immune system, such as T-cells and neutrophils, and other substances. In some cases, this “outsiders” can cause cell damage, subsequently triggering a neuroinflammatory response and leading to the activation of glial cells, which further propagate the inflammatory response[69,70]. In short, this self-propagating process is characterized by molecules that attract and activate other cells to participate in an inflammatory response, including cells form the peripheral immune system, that in turn produce more inflammatory substances of their own, further exacerbating the reaction and eventually causing a chronic neuroinflammation that leads to cell damage and death[71].

1.1.2.5.1. Microglia

Microglia are the residing immune cells of the brain. These cells have several functions, but mainly monitor the diverse brain regions, maintaining the homeostasis and assuring the proper development and neuroprotection of the CNS[28,72,73]. In a normal environment, these cells adopt a ramified appearance, characteristic of their resting state, where they control the integrity of the dendritic spines and remodel neural circuits[28,72]. When the environment is disturbed through lesions, infections or other noxious events, microglia become activated, being a crucial participant in the resolution of the threat[28,73]. Yet, in some cases they can become over-activated, excessively producing cytotoxic factors which end up potentiating neuroinflammation, and ultimately harming the environment they are intended to protect[28,74]. In addition, as more microglia become activated, less individuals remain to monitor the synapses, leading to disturbances of the neuronal circuits[28,74].

The activation of NLRP3 inflammasome leads microglia to alter its morphology to the activated pro-inflammatory M1 phenotype[38], triggering the cell to produce and release a set of pro-inflammatory cytokines that participate in neuroinflammation, including IL-1β, tumour necrosis factor alpha (TNFα), IL-6, IL-18 and gamma interferon (IFN-γ), and producing nitric oxide (NO), ROS, and many others associated with neurodegeneration[28,75]. In the context of AD, it was shown that when the inflammasome is dysfunctional, microglia adopt the neuroprotective M2 phenotype[38].

It is also suggested that the degeneration of neurons release tau aggregates that further affect glial cells[28]. Microglia captures both soluble and insoluble forms of tau and Aβ, which once engulfed can be either degraded or released in exosomes to the extracellular space[76-78]. When phagocytosed, Aβ peptides can cause the lysosomes that contain them to swell, subsequently damaging its structure[79]. Eventually, microglia become unable to efficiently degrade Aβ and the lysosome contents, like cathepsin B, are leaked into the cytosol, where they trigger the inflammatory response[80]. In addition, augmented levels of exosome-associated tau were found in the CSF of AD patients[81], suggesting that microglia may actively contribute to non-synaptic tau propagation. This hypothesis was strengthened by another study that inhibited exosome synthesis, in turn reducing tau secretion from microglia *in vivo*, thus halting the development of the tau pathology[76]. However, this work presented some limitations such as the low number of animals tested and it only examined p-tau species, not fibrillar aggregates. Therefore, further investigation is needed to fully understand the relation of microglia-derived exosomes and the development of the tauopathy.

An increasing number of studies have been highlithing the role of NLRP3 inflammasome in neuroinflammation, strengthening its impact over the progression of the disease[38,79,82]. The many requirements and activation steps involved in the process, along with the transport in exosomes highly increase the dynamics of neuroinflammation.

1.1.2.5.2. Astrocytes

Astrocytes are the most abundant type of cells in the brain. These cells are an integral part of the "tripartite synapse"[4], a term used to describe the bidirectional communication between neurons and astrocytes, contributing to the modulation of synaptic transmission and plasticity through the release of gliotransmitters (such as glutamate, GABA, ATP, TNFα, etc)[83], and through the adjustment of extracellular concentrations of ions and neurotransmitters. This complex interaction has been identified in brain structures such as cortex and hippocampus, which explains its impact upon memory and learning[4,84]. Astrocytes play crucial roles in the organ's development and function,

synaptogenesis, structural support, maintenance of the BBB, neuronal metabolism and immune responses[4,84-86].

The fibrous astrocytes contact with blood capillaries and axons, being mainly predominant in the white matter, whereas the protoplasmic ones are predominant in the gray matter, near synapses and blood capillaries[87]. As described for microglia, this group of macroglia becomes activated in response to CNS insults. They present reversible alterations in gene expression, hypertrophy of the cell body, thickness of their processes and ultimately, the formation of a glial scar, which attempts to isolate the threat[87]. Furthermore, two types of reactive astrocytes were recently described, the A1 and A2[69,87]. The A1 astrocytes are considered neurotoxic, are common in neuroinflammatory conditions and often show increased expression of pro-inflammatory genes that end up compromising synapses[4,69,87]. It was recently shown that microglia released factors (IL-1α, TNFα and C1q) can stimulate astrocytes reactivity to the A1 phenotype[88,89]. On the contrary, A2 astrocytes are induced by ischemic conditions and contribute to neuronal survival and growth as they promote the expression neuroprotection-related genes[69,87]. Classical hallmarks of neuroinflammation include the increase in the expression of Glial fibrillary acidic protein (GFAP), which is an indicator of astrocytic reactivity and is expected to increase with the progression of reactive astrogliosis. Upregulation of complement component 3 (C3), and of C3 cleavage products, like C3d, was described in A1 astrocytes[90,91].

Expression of activator protein 1 (AP-1), NF-κB, some mitogen-activated protein kinase (MAPK) pathway constituents and Ca^{2+}/calmodulin-dependent protein phosphatase calcineurin, by astrocytes, makes the cell highly sensitive to IL-1β levels[88]. For instance, interaction of IL-1β with membrane receptors such as receptor for advanced glycation endproducts (RAGE) or IL-1R, triggers a pathway that ultimately leads to the translocation of NF-κB to the nucleus where it activates genes that encode for pro-inflammatory chemokines, adhesion molecules and cytokines such as IL-1β, IL-6 and TNFα, thus perpetuating the inflammation[4,92].

Undeniably, astrocytes are important players in the neuroinflammatory processes. Regarding the involvement of astrocytes in AD, from a

neuroinflammatory perspective, there are several evidence that suggest an important role for these cells. To begin, they are the major producers of ApoE[30], the principal lipid transporter of the CSF. There are three main isoforms of ApoE (ApoEε2, ApoEε3, and ApoEε4), and *in vitro* experiments showed that astrocytes containing the ApoEε4 allele were less effective eliminating Aβ plaques than those astrocytes expressing the ApoEε3 allele[30]. In fact, the presence of the ApoEε4 allele is considered a risk factor in AD, whereas the presence of ApoEε2 allele is considered a protective factor[30,90].

Under normal physiological conditions, this cell can recur to CD36, CD47, and RAGE mediated phagocytosis to eliminate Aβ peptides, thereby helping to restore impaired neural circuits and reducing the inflammatory impact of damaged neurons[42]. However, a study showed that internalization of high amounts of Aβ protofibrils by mice astrocytes, may cause incomplete digestion to occur, which in turn results in an increased intracellular toxicity caused by truncated forms of Aβ, and also lysosomal dysfunction[93].

Furthermore, over the last years, many studies have identified several pathways through which Aβ is able to compromise crucial roles played by astrocytes. Both chronic and acute exposure to this peptide have shown to be able to disrupt gliotransmission by enhancing Ca^{2+} signalling, either by increasing its release from the endoplasmic reticulum or by interacting with receptors such as P2Y1, nicotinic receptors (such as α7nAChR) and metabotropic receptors (such as mGluR5)[84]. The increased Ca^{2+} intracellular levels can cause glutamate release, leading to excessive stimulation of N-methyl-D-aspartate (NMDA) receptors in neurons, ultimately giving rise to excitotoxicity[84]. Having a high-lipid and poly-unsaturated fatty acids content, and a low concentration of antioxidants, the brain is particularly susceptible to lipid peroxidation and consequently oxidative stress[94]. Aβ is known to induce the production of ROS and reactive nitrogen species (RNS), which increase oxidative stress and affect cellular mechanisms such as intracellular calcium levels, NADPH oxidase (NOX), NF-κB signalling, mitochondrial function and glutamate uptake, again increasing the risk of excitotoxicity[4]. Also, the release of Ɣ-aminobutyric acid (GABA) by reactive astrocytes can augment dysfunctions related with synaptic plasticity, and cognitive functions in APP/PS1 mice[95]. In fact, increased levels of GABA and

monoamine oxidase B were found predominantly in reactive astrocytes of brains from *postmortem* AD patients[95].

1.1.2.6. Cell Death by Pyroptosis

Pyroptosis is a recently described type of programmed cell death dependent on Caspase activation, especially Caspase-1[37]. Recent studies have shown that pyroptosis is associated with a variety of neurodegenerative diseases due to its pro-inflammatory effect and related cell dysfunction[96]. Morphologically, pyroptosis is characterized by the formation of pores in the plasma membrane and rupture of the same, leading to the release of inflammatory cytokines IL-1β and IL-18 and other DAMPS, thus spreading the inflammatory effect, unlike apoptosis that does not rupture the plasma membrane (**Fig. 6**)[97,98].

In addition to the role of maturing pro-inflammatory cytokines, Caspase-1 also promotes the cleavage of the pore forming protein Gasdermin D (GSDMD)[99]. When the cleavage occurs, the N-terminal fragment (GSDMD-NT) is formed, and subsequently translocated to the inside of the plasma membrane, where it binds to phosphatidylinositol phosphates and phosphatidylserine, thus oligomerizing and originating pores, giving rise to pyroptosis[99,100]. To support this evidence, a study suggested that GSDMD-NT is capable of triggering pyroptosis on its own, after observing that pyroptosis-inducing activity of GSDMD-NT was inhibited when the NT terminal was linked to the C-terminal (GSDMD-CT)[101]. Another study revealed that GSDMD-NT can also combine with liposomes to form membrane pores[102].

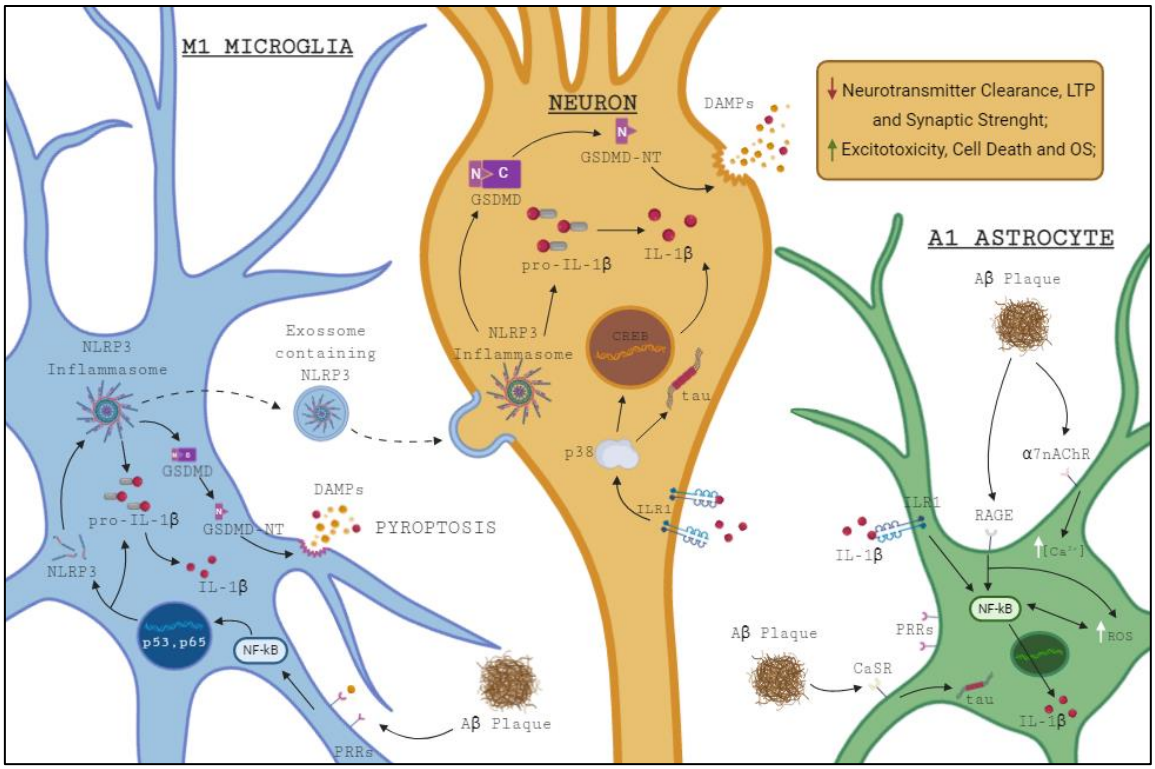

Figure 6. Cellular death by pyroptosis. This figure summarises the concepts previously explained and that can have an impact on pyroptosis. Aβ oligomers trigger glial cells to produce inflammatory cytokines via NLRP3 inflammasome-mediated Caspase-1 activation, and releasing them to contact with neighbouring cells, thus perpetuating the inflammatory response. Neurons can also capture microglial derived vesicles containing NLRP3 domains. Ultimately pro-Caspase-1 is cleaved into active Caspase-1, which acts upon GSDMD, releasing the GSDMD-NT that opens pores in the cell membranes from within, allowing the leakage of the intracellular content and initiating pyroptosis.

2. Aims

AD is a scourge that affects millions of elders worldwide, with dire consequences in each of their lives and the lives of their dear ones. The lack of reliable biomarkers and treatment availability in such a devastating disease makes it urgent to map its processes and mechanisms, as best as possible, so that new therapeutical targets may rise, especially ones that target the disease in its early stages and that can halt its progression or even prevent it.

MCC950 has been highlighted as a selective inhibitor of NLRP3 inflammasome activation in several inflammatory diseases. Authors have proven the potential of MCC950 in weakening inflammatory diseases, however, no one has ever suggested MCC950 as a possible preventive therapy to be adopted by people entering the risk age. In AD animal models, this inhibitor has been shown to decrease the deposition of Aβ, decrease microglial activation and IL-1β release, together with an increase in cognitive function[37,40,64].

Therefore, this project has two aims: 1) to characterize the neuroinflammatory milieu in a model of Aβ-induced toxicity in acute slices, and 2) to evaluate the potential protective effect of MCC950 upon Aβ impact.

To achieve these goals several topics will be evaluated in acute hippocampal slices:

- Expression profile of resting/reactive glial cells;
- Expression profile of NLRP3 inflammasome domains (NLRP3, ASC, Caspase-1) and related proteins (Gasdermin D);
- Evaluation of IL-1β release.

3. Materials and Methods

3.1. Ethics Statement

Portuguese law and European Union guidelines (2010/63 / EU) were respected in all procedures related to the protection of animals for scientific purposes. Every effort was made to minimize animal suffering and use the minimum number of animals. Additionally, this study is approved by the institutional animal ethics committee, "Órgão Responsável pelo Bem-Estar Animal" - ORBEA-IMM, and by the competent national authority - DGAV (Direção Geral de Alimentação e Veterinária).

3.2. Compounds

In this work the 42-aminoacid isoform of Aβ was used as it has been proven to be present in the brains of AD patients, and because it is the most neurotoxic of all Aβ variants[18,19]. $A\beta_{1-42}$ was acquired from Bachem (Bubendorf, Switzerland) and used to prepare a stock solution of oligomers (120 µM) through a specific protocol[103-106]. Briefly, $A\beta_{1-42}$ (1 mg/ml) was resuspended in Phosphate-Buffer Saline solution (PBS: NaCl 137 mM, KCl 2.7 mM, $Na_2HPO_4.2H_2O$ 8 mM, KH_2PO_4 1.5 mM, pH 7.4), supplemented with 0.025% ammonia solution and adjusted to a final pH 7.2. Species separation was based on an ultrafiltration process[107]. Then, Aβ (220 µM) was allowed to oligomerize by constant shaking at 600 rpm, at 37 ºC for 16 h and ultracentrifuged (40000g, 30 min) for separation of fibrils (pellet). Supernatant was further separated in centrifugal filters (30 kDa Amicon Ultra). The concentration of the retained fraction, corresponding to oligomers >30kDa, was spectrophotometrically determined ($\varepsilon 280=1490\ M^{-1}cm^{-1}$).

As it is very prone to aggregation, this compound was always stored at -80 ºC and its transport made always on ice. $A\beta_{1-42}$ oligomers were used at 200 nM[105,107], diluted from stock solution in an artificial cerebrospinal fluid (aCSF: glucose 10 mM, NaCl 124 mM, KCl 3 mM, NaH_2PO_4 1.25 mM, $NaHCO_3$ 26 mM, $CaCl_2$ 2 mM, $MgSO_4$ 1 mM in distilled water).

The small molecule inhibitor MCC950, with the chemical formula $C_{20}H_{23}N_2NaO_5S$, was bought from AdipoGen (Liestal, Switzerland, ref. AG-CR1-3615-M005). The stock solution was prepared in Milli-Q water at a concentration of 23,4 mM and stored at -20 ºC. MCC950 was used at 1 µM prepared in aCSF, a concentration known to exert effect upon NLRP3[63].

Isoflurane (Isoflo®, Barcelona, Spain) was the anaesthetic and analgesic used, through inhalation, for the sacrificing procedure.

3.3. Animal and Housing

For this study young male Wistar rats, 7-8 weeks old, were used. The animals were purchased from Charles River Laboratories (Lyon, France) and after arriving at IMM, in groups of 4-6 individuals, they were housed together and left acclimatizing at least for 5 days. In addition, the animals were housed in a room with controlled light and temperature conditions (20 ± 2 ºC; lights on between 6 a.m. and 7 p.m.) and had unlimited access to food and water.

3.4. Dissection and Preparation of Acute Slices

Firstly, aCSF was left oxygenating for 15 min with a continuous source of 95% O_2 and 5% CO_2. During this time, the dissection material and Mcilwain Tissue Chopper cutting apparatus were prepared.

It is highly important to perform the brain dissection on ice, to preserve the tissue and stop the metabolism, and so the aCSF solution was frozen on liquid nitrogen and continuously rubbed with a spatula until it formed an “ice paste”. Once the rat was anesthetised with 1-1,5 ml of isoflurane (shows no reflex), it was sacrificed with a guillotine. The brain was quickly removed and placed on ice-cold aCSF. The hippocampus was isolated and cut in 400 µm hippocampal slices in the tissue chopper. Slices were incubated at room temperature (RT), for 1 hour, to resume their metabolism.

The slices were then carefully transferred with a Pasteur pipette to a homemade 6-well incubation chamber, in a proportion of 5 slices per well, each

well representing a single condition. Freshly oxygenated aCSF (2 ml) and the previously prepared MCC950 were added to the respective wells. At the end of the first hour of incubation, $A\beta_{1-42}$ oligomers were added to the respective wells. The remaining 4h incubations proceeded according to **Fig. 7**, at RT and with a continuous source of 95% O_2 and 5% CO_2.

Overall, four conditions were tested: **control** (CTL), slices maintained in oxygenated aCSF; **Aβ**, slices incubated with of $A\beta_{1-42}$ oligomers (200 nM) from the second hour of incubation until the fifth; **MCC950,** slices incubated with MCC950 (1 µM); **MCC950 + Aβ,** slices incubated with MCC950 (1 µM) and $A\beta_{1-42}$ oligomers (200 nM) (**Fig. 6**).

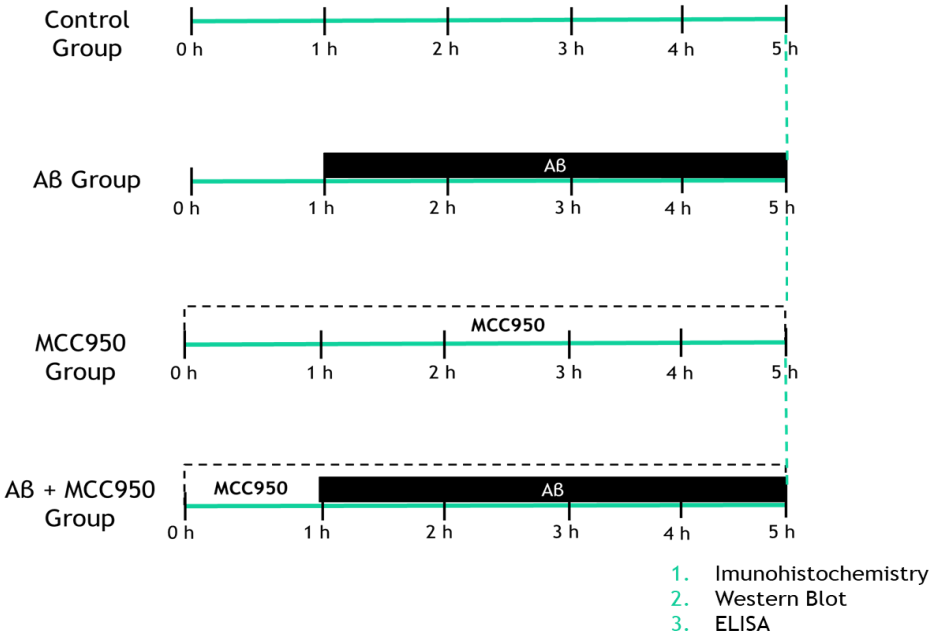

Figure 7. Experimental conditions. Representation of the four experimental conditions used, organized by groups, each occupying a different well in the 6-well incubation chamber. CTL, slices maintained in aCSF; Aβ, slices incubated with of $A\beta_{1-42}$ oligomers (200 nM) from the second hour of incubation until the fifth; MCC950, slices incubated with MCC950 for 5h (1 µM); MCC950 + Aβ, slices incubated with $A\beta_{1-42}$ oligomers (200 nM) in the presence of MCC950 (1 µM). MCC950 incubation started 1h earlier than $A\beta_{1-42}$ oligomers incubation.

It is known that the lifespan of acute brain slices is approximately 6 to 12 hours. However, as they are incubated in a non-sterile environment, they are exposed to environmental dangers which can decrease cell viability[108].

Therefore, the 5-hour incubation time has been set as the optimal time to perform an acute exposition to Aβ, and at the same time avoiding significant contamination risk.

Finally, slices were processed according to their destination. If they were to be tested for Western Blot (WB) or Enzyme Linked ImmunonoSorbent Assay (ELISA), the medium and tissue, respectively, were collected to separate tubes and immediately frozen at -80 ºC. However, if they were to be used in immunohistochemistry (IHC) assays they would be fixed in a 4% paraformaldehyde (PFA) solution and subsequently in 30% sucrose, as soon as the 5 hours of incubation ended.

For the validation of the Aβ-induced toxicity in acute slices, only CTL and Aβ conditions were used. To evaluate the efficacy of MCC950 in halting the Aβ-induced neuroinflammatory context all experimental conditions were prepared. Regarding the assays, for the first part of the project only WB and ELISA were performed, whereas for the second part all three assays were applied WB, ELISA and IHC.

3.5 Protein Extraction from tissue with Lysis Buffer

To perform the Western Blot assays and ELISA the tissue that was stored at -80 ºC after dissection was processed. In this process it is important to always maintain the tissue on ice to stop any metabolic reactions.

120 µl of complete Lysis Buffer (cLB: Tris 50 mM pH 8.0, EDTA 5 mM, NACl 150 mM, 1% NP-40, 5% Glycerol), supplemented with protease inhibitors (cOmplete™, Mini, EDTA-free Protease Inhibitor Cocktail; Roche, Basel, Switzerland) and Phenylmethylsulfonyl fluoride (PMSF, 1 mM) were added to the tissue and dissociation took place in a sonicator (W-225, Heat Systems-Ultrasonics). The resulting suspension was transferred to microtubes, and after incubating at 4 ºC with slow agitation for 15 min, they were centrifuged at 13 000g for 10 min at 4 ºC. The resulting supernatant was removed to new microtubes and was either stored at -20 ºC or processed for total protein quantification.

3.6 Protein Quantification

To determine the protein concentration of each homogenate prepared, the Bradford assay was performed, using the Bio-Rad DC™ Protein Assay kit (Bio-Rad Laboratories, California, USA) and according to section 5 of DC Protein Assay Instruction Manual.

Briefly, a calibration curve, ranging from 0 to 1 mg/ml, was prepared by diluting a Bovine Serum Albumin (BSA) stock solution. Afterwards, 10 µl of both standard and samples (diluted 1:20) were added to a 96-wells flat bottom plate. All dilutions were made in Milli-Q water. After 15 min in slow agitation, absorbances were read at 750 nm in the Microplate Reader TECAN Infinite M200 (Tecan, Männedorf, Switzerland).

3.7. Enzyme Linked Immunosorbent Assay (ELISA)

ELISA is based on antigen-antibody reactions detectable through enzymatic reactions, particularly immunoenzymatic tests[109].

This work used a sandwich ELISA where two antibodies, capture antibody (CA) and detection antibody (DA), are employed[109-111]. The first antibody must be selected for a specific antigen, in this case IL1β, and immobilized against the surface of a 96-well microplate. Afterwards, the biological sample is added to the wells, where the antigen of interest with bind to the CA. Subsequent washing steps wash away the remaining non-attached substances. In the next step DA, an enzyme-tagged antibody also designed to bind to the antigen of interest, is added. Finally, enzyme-specific substrates, such as horseradish peroxidase (HRP), are added to the plate, reacting with the enzyme and producing a coloured product for detection[109].

To determine the antigen concentration of the target, a standard curve is created using known concentrations of the antigen. Then, a colorimetric assay is performed, requiring a microplate reader to obtain the optical densities, consisting of the light absorption of the enzyme-substrate reaction product, which are plotted on the standard curve to measure exactly the antigen level in the biological sample[109].

ELISA is highly sensitivity and specific, suitable for detecting target molecules at picogram levels. However, the time for detection is very short as the quantification is based on an enzyme-substrate reaction. In addition, this assay only informs about the presence or amount of a certain substance, and not its location and distribution[109].

3.7.1. ELISA Protocol

This assay was performed following the manufacturer's protocol kit (DY008, Human IL-1 beta DuoSet ELISA, R&D Systems, Minnesota, USA). In the first day, the washing buffer (WB - 0,05% Tween 20 in (PBS), pH 7,2-7,4), reagent diluent (RD – 1% BSA in PBS, pH 7,2-7,4) and the CA (0,8 µg/ml) were prepared. The WB and RD were stored at 4 ºC, while 100 µl of the CA were added to each well of a 96-well plate, that was covered with an adhesive and left incubating overnight at RT.

On the second day the WB and RD were removed from their 4 ºC storage and allowed to acclimatize for 30 min. Then, the CA was removed from the wells and 400 µl of WB were added to each well in order to wash the excess CA that did not adhere to the well's surface (this washing procedure was performed three times).

Afterwards, for the blocking step, 400 µl of RD were added to each well, and the plate was left incubating for 1h. During this hour of incubation, the standard and samples were prepared. The two-fold standard serial dilutions (ranging from 1,95 to 1000 pg/ml), were prepared in cLB.

The next step was the addition of 100 µl of the samples and standard dilutions to the respective well, followed by a 2h incubation at RT. During this time the DA (0,1 µg/ml) was prepared. After the incubation, the washing procedure was performed once again and 100 µl of DA was added. Subsequently, while the plate was left incubating for 2h at RT, the HRP solution was prepared and agitated for 15 min (hidden from light). Once the 2h ended, and after three washes the plate was incubated for 20 min with 100 µl of the HRP solution in each well. From this step onwards, the plate was always covered from light.

During the incubation of HRP, the substrate solution was prepared with reagents A (H_2O_2) and B (Tetramethylbenzidine). When the incubation ended, three washings with WB were performed and 100 µl of the substrate solution was added to the wells. After another incubation of 20 min, the reaction was stopped with 2N of sulfuric acid (H_2SO_4). Absorbance was read at 450 nm with a 540 nm reference in the Microplate Reader TECAN Infinite M200.

3.8 Western Blot (WB)

Western blotting or protein immunoblotting originated in 1979[112] and has become a routine technique widely used in molecular biology for protein analysis. With this technique, it is possible to obtain information about the molecular mass and the relative quantity of a specific target[113,114].

WB is based on the separation of proteins by molecular weight through electrophoresis, followed by the transfer to a membrane and the detection of the protein of interest with a specific antibody[113,114]. There are five steps to develop this technique: protein extraction and quantification; polyacrylamide gel electrophoresis (PAGE); transfer of proteins to a membrane; incubation of the membrane with antibodies to detect the specific protein to be analysed and chemiluminescent detection of the membrane for data analysis[113,114].

In this work the expression profile of several proteins was evaluated, namely:

i. **GFAP** marker**,** to detect astrocytes and observe their morphologies[115];
ii. C3 cleavage product **C3d**, known to be upregulated in reactive (A1) astrocytes due to uncontrolled complement cascade activation [89,91];
iii. Ionized calcium-binding adaptor molecule 1 **(Iba-1)**, marker of resting and reactive microglia, which allows to observe microglia morphology[116];
iv. Cluster of Differentiation 68 **(CD68)**, a lysosomal protein, upregulated in reactive microglia[117,118];
v. **NLRP3,** the intracellular sensor of NLRP3 inflammasome[119,120];

vi. **ASC**, the NLRP3 inflammasome adaptor that binds NLRP3 domain to pro-Caspase-1;

vii. **Caspase-1**, the NLRP3 inflammasome effector [36,38,41,54,75,120-122];

viii. GSDMD, to evaluate the presence of the full-length form (**FL-GSDMD**) and the cleaved one (**GSDMD-NT**), marker of cell death by pyroptosis[99,100];

ix. Glyceraldehyde-3-phosphate dehydrogenase **(GAPDH),** the enzyme that belongs to the group of the so called “housekeeping proteins”, being constitutively expressed in almost all tissues in high amounts. For this reason, GAPDH is widely used as a loading control for protein normalization in WB.

3.8.1 Sodium dodecyl sulphate-polyacrylamide gel electrophoresis (SDS-PAGE)

Firstly, the Bio-Rad apparatus was assembled, followed by the preparation of the 12% resolving and 5% stacking gels. The latter is used to load 45 µg of sample protein per lane, whereas the first, being much larger, is used to separate the proteins according to their size, meaning that smaller proteins migrate faster towards the positive pole of the run. Both gels contain SDS as it denatures folded proteins, allowing them to travel more easily through the gel, as well as assigns a negative charge to them. The molecular weight marker (MWM, NZYColour Protein Marker II, NZYTech, Lisboa, Portugal) was used. Samples were diluted in loading buffer, which contained a tracking dye (bromophenol blue) to allow the electrophoresis to be monitored.

Samples (45 µg of total protein per lane) were denatured at 100 ºC for 10 min and kept on ice. At this point, samples and the MWM were applied to the wells and the gel was run at 80 volts until it reached the resolving gel. At that moment, the voltage was increased to 120 volts and the run continued for 1h 30 min.

Separated proteins were then electrotransferred at 350 mA for 100 min to polyvinylidene fluoride (PVDF) membranes (GE Healthcare, Buckinghamshire,

UK), previously activated with fresh methanol in order to increase its affinity towards the proteins.

3.8.2 Chemiluminescent Detection and Densitometry Analysis

As the transfer ended, the membranes were blocked with a 3% BSA in Tris Buffer Saline with Tween-20 (TBST: Tris base 20 mM; NaCl 137 mM; 0.1% Tween-20) for 1h with small agitation at RT, to avoid future non-specific antibody binding. After the blocking step, the membranes were washed three times, 10 min each, with TBST, and incubated overnight at 4 ºC with the primary antibody, diluted in 3% BSA (Table 1). In the following morning, anti-mouse, anti-rabbit or anti-goat HRP-conjugated antibodies (all from Bio-Rad), diluted 1:10000 in blocking solution, were added to the membranes for 1h at RT with small agitation (Table 2).

After a washing step, immunoreactions were visualized using the ECL Western Blotting Detection System (Cytiva (Formerly GE Healthcare Life Sciences) Amersham ECL Prime Western Blotting Detection Reagent, Buckinghamshire, UK). Chemiluminescence was developed and detected in Image Lab software 6.0.1 associated to the ChemiDocTM XRS^{+} System (Bio-Rad, California, USA). Membranes were re-probed with different antibodies, after a 30 min period incubation in stripping solution (200 mM glycine, 0.1% SDS, 1% Tween 20, 50% acetic acid glacial, pH 2.2).

The integrated intensity of each band was calculated using computer-assisted densitometry analysis with ImageJ software 1.52a. The image chosen for quantification was the one just before signal saturation. GAPDH was used to normalise band intensities, correcting possible loading errors. All integrated intensities were normalised to GAPDH and finally to the CTL condition. The representative image of each protein evaluated was prepared in Image Lab by merging the chemiluminescence image with the colorimetric image of the MWM.

Table 1. Primary antibodies used in Western Blot

PRIMARY ANTIBODY	ANTIGEN (kDa)	COMPANY	WORKING DILUTION
Rabbit anti-NLRP3	118	Abcam: ab214185	1:300
Rabbit anti-ASC	22	Apidogen: AG-25B-0006	1:1000
Rabbit anti-Caspase-1	20	Biotechne: NBP1-4533SS	1:400
Rabbit anti-GSDMD	53 / 32	Abcam: 209845	1:400
Goat anti-C3d	34	R&D Systems: AF2655	1:500
Rabbit anti-GFAP	50	Sigma: G9269-.2ML	1:5000
Mouse anti-CD68	37	Abcam: 31630	1:500
Goat anti-Iba1	17	Abcam: ab5076	1:500
Mouse anti-GAPDH	36	Ambion: AM4300	1:5000

3.9 Immunohistochemistry (IHC)

Immunohistochemistry, as WB, is a method that explores the principle of specific antibodies binding to antigens (e.g., proteins) in biological tissue. Specific molecular markers are characteristic of cell events, such as cell proliferation or death, but IHC is also widely used in basic research to understand the distribution and location of biomarkers and proteins differently expressed in different parts of biological tissue. The value of this technique for structural studies is widely recognized, being considered a pillar in biomedical research for many different fields of science, including neuroscience, where it is key for the understanding of the brain's cellular architecture, organization and interactions, and also for the study of neuropathologies[123-125].

3.9.1 IHC Protocol

After the dissection and subsequent incubations, the slices obtained were placed in a 6-well plate and fixed with 4% PFA overnight. Fixing ensures that sample cell structures stay intact and that antigens are immobilized, while ideally still permitting unfettered access of antibodies to target antigens[126]. In the following morning, PFA was removed and the slices were incubated with increasing concentrations of sucrose in PBS, starting with 15% for 2h and then 30% overnight at 4 ºC[127]. The purpose of cryopreserving tissues with sucrose is to help prevent ice crystal formation in tissues when water freezes and expands. Ice crystals break cell membranes and produce holes within cells and loose extracellular matrix. Slices were kept in 30% sucrose until delivery to the Histology and Comparative Pathology Laboratory of IMM, where they were cut into 40 µm sections through a process of cryosection and placed on a microscope slide. From this point on, the samples were stored at -20 ºC[127], until further processing.

At the day of the experiment, slides were removed from their -20 ºC storage and placed at RT in PBS for 10 min. Then, to remove the gelatine added during the cryosectioning procedure, the slides were placed in PBS at 37 ºC for 20 min, and finally they were transferred back to PBS at RT. Afterwards, the slides were removed from the PBS and the excess of this solution was carefully removed with a tissue in order to allow each section to be surrounded with a hydrophobic pen (Dako, Glostrup, Denmark). After this step, the PFA residues were washed with a freshly prepared 0.1M glycine in PBS solution for 10 min are RT, followed by a permeabilization step with 1% Triton in PBS for 1h at RT. Slices were blocked with 10% donkey serum and 6% BSA for 2h at RT.

The permeabilization step using detergent ensures that large antibodies can enter the cell and bind intracellular targets and the blocking step was performed to reduce nonspecific antibody binding. Once the permeabilization and blocking have occurred, sections were incubated with the corresponding primary antibodies, diluted to the working dilution in PBS, overnight at 4 ºC (140 µl of antibody solution per section).

Sections were then washed three times, for 10 min each time, with PBS with 0.1% Tween-20 (PBSTw). Subsequently, sections were incubated with the Alexa Fluor-488/568 coupled secondary antibodies (diluted 1:200, Invitrogen) for 1h at RT. Considering that secondary antibodies have fluorophores accoupled, from this step on, slides were protected from light and left incubating.

At the end of the incubation, sections were washed three times, for 10 min each time, with PBSTw. Then, 50 µl of the nuclear marker HOESCHT (20 µmg/ml) were added on each section and left incubating for 10 min at RT. After three washes, for 10 min each time, with PBSTw, and one last wash with PBS in order to remove potential bubbles sections were covered with Mowiol, followed by the addition of a coverslip. Finally, to seal the complex, preventing it from drying, nail polish was added around the edges of the coverslip and it was left to dry for 24 hours. With the immunohistochemistry procedure complete, the stained sections were stored at -20 ºC until they were visualized under LSM 880 Zeiss confocal microscope.

3.9.2 Attempts in immunohistochemistry assays

Immunohistochemistry assays were attempted to corroborate the WB results. Unfortunately, further optimizations are still required, since confocal images had a lot of unspecific binding and no clear images could be obtained.

3.9.2.1 Reactive gliosis

To visualize the impact of MCC950 upon the reactive astrogliosis induced by $A\beta_{1-42}$ oligomers a double staining of GFAP and C3d was attempted, whereas a double staining of Iba-1 and CD68 was struggled to address the Aβ-induced microglia phenotypes and the impact of MCC950 upon them. The primary antibodies used were mouse anti-GFAP (1:500, MAB360, Millipore SAS), goat anti-C3d (1:1000, AF2655, R&D Systems), rabbit anti-Iba-1 (1:500, ab108539, Abcam) and mouse anti-CD68 (1:250, ab31630, Abcam).

3.9.2.2 Neuronal death by pyroptosis

WB assays do not allow to discriminate which cell type was affected by pyroptosis. To assess the occurrence of Aβ-induced neuronal death by pyroptosis, and also the impact of MCC950 upon this event, a double staining of

the neuronal marker NeuN and GSDMD was attempted. The primary antibodies used were mouse anti-NeuN (1:500, MAB377, Millipore SAS) and rabbit anti-GSDMD (1:200, ab209845, Abcam).

3.10 Statistical Analysis

For the validation of the model of Aβ-induced toxicity in acute slices, statistical analysis was performed using Students' t-test. In the remaining experiments, statistical analysis was performed with one-way Analysis of Variance (ANOVA) followed by a Holm-Šídák's multiple comparison test. All analyses were performed using GraphPad Prism software 8.0.2 (GraphPad Software Inc). Results are expressed as mean ± standard error of the mean (SEM). Statistical significance was considered when $p<0.05$.

4. Results

4.1. Impact of $A\beta_{1-42}$ oligomers on the neuroinflammatory milieu

There are many animal models of AD, which use transgenic mice and rats, zebrafish, fruit flies (Drosophila melanogaster) and even non-human primates[128]. However, simpler models offer excellent tools to screen potential therapeutic targets. As so, we decided to test the preventive effect of MCC950, the selective NLRP3 inflammasome inhibitor, on the neuroinflammatory milieu induced by Aβ in acute hippocampal slices.

First, the neuroinflammatory context induced by $A\beta_{1-42}$ oligomers was characterized in a model of Aβ-induced toxicity in acute hippocampal slices. Hippocampal slices incubated in aCSF for 5h (CTL group) were compared with slices maintained in the presence of 200nM of $A\beta_{1-42}$ oligomers ($A\beta_{1-42}$ condition) from the second to the fifth hour, as represented in **Fig. 7**.

4.1.1. $A\beta_{1-42}$ oligomers induce reactive gliosis

$A\beta_{1-42}$ oligomers are known to trigger inflammatory cascades that cause continuous cell death and neuronal dysfunction[26]. The protagonists of this response are the glial cells, specifically microglia and astrocytes, through a process named reactive gliosis. The activation of astrocytes is characterized by an upregulation of GFAP and C3d, while microglia activation is accompanied by an increase in Iba-1 and CD68 markers. Thus, the expression of these proteins was evaluated through WB.

As depicted in **Fig. 8**, the expression of GFAP and C3d is significantly increased in $A\beta_{1-42}$ condition (GFAP: 1.38 ± 0.11, $p<0.01$; C3d: 1.33 ± 0.09, $p<0.01$) when compared to CTL condition, pointing to an Aβ-induced astrogliosis. Similarly, as shown in **Fig. 9**, Aβ also induces microglia activation since a significant increase in CD68, a marker for reactive microglia, is observed in the presence of $A\beta_{1-42}$ oligomers (1.33 ± 0.08, $p<0.01$). Regarding Iba-1 expression no significant differences were found between $A\beta_{1-42}$ and CTL conditions (1.16 ± 0.11, $p>0.05$).

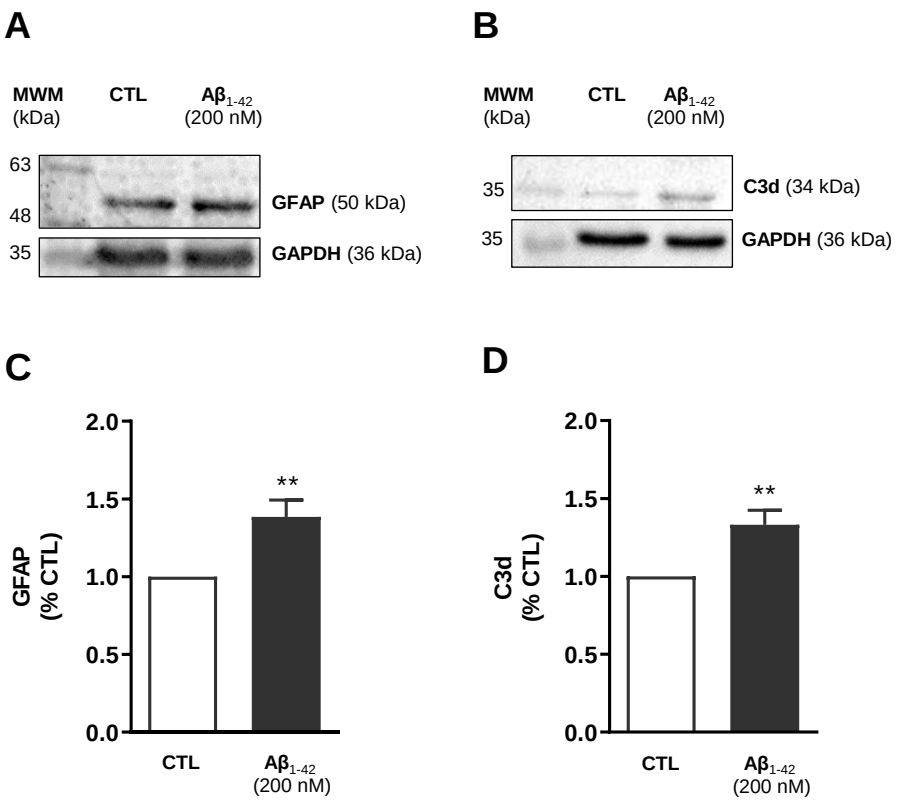

Figure 8. $A\beta_{1-42}$ oligomers induce astrogliosis in hippocampal slices. Representative immunoblots of **(A-B)** GFAP, C3d and GAPDH in CTL and Aβ-incubated slices. Densitometry analysis of **(C)** GFAP and **(D)** C3d was performed with ImageJ software using GAPDH as the loading control. Results are presented as percentage of CTL slices. There was a significant increase in GFAP and C3d in Aβ-incubated slices compared with CTL ones. All values are mean ± SEM. N=6-7 independent experiments. Statistical tests were performed with *t*-test, **p<0.01.

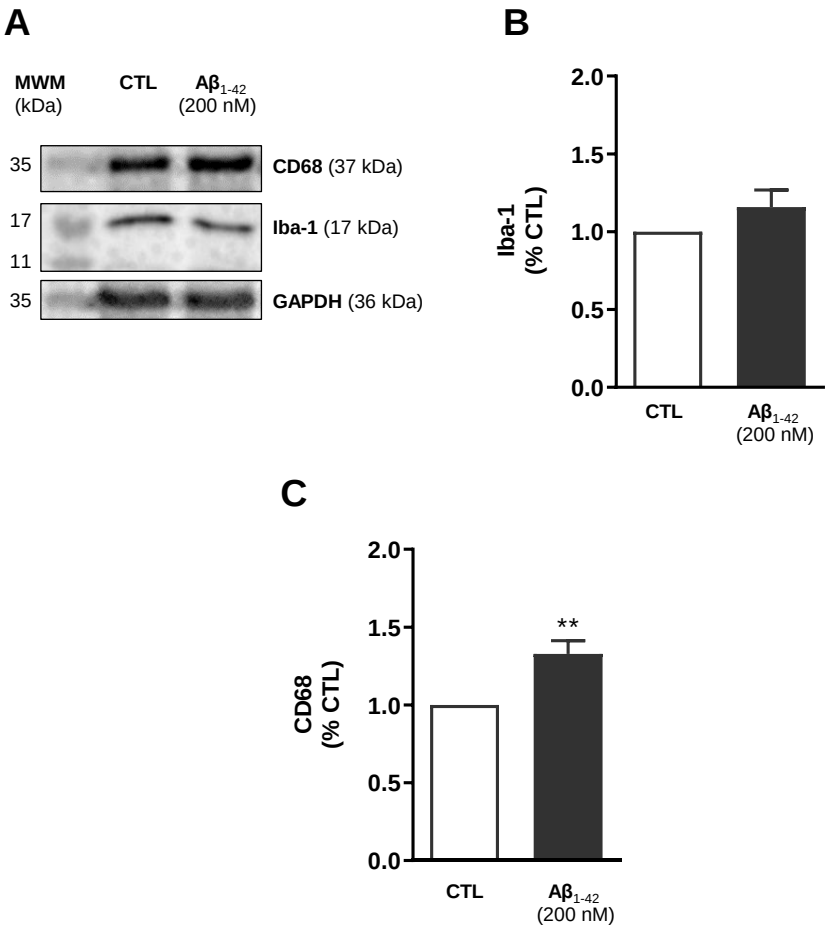

Figure 9. $A\beta_{1-42}$ oligomers induce microglia activation in hippocampal slices. (A) Representative immunoblots of Iba-1, CD68, and GAPDH in CTL and Aβ-incubated slices. Densitometry analysis of **(B)** Iba-1 and **(C)** CD68 was performed with ImageJ software using GAPDH as the loading control. Results are presented as percentage of CTL slices. There was a significant increase, compared to CTL slices, in Aβ-incubated slices regarding CD68 expression, but no significant changes were observed in Iba-1. All values are mean ± SEM. N=7 independent experiments. Statistical tests were performed with *t*-test, **p<0.01.

4.1.2. $A\beta_{1-42}$ oligomers induce changes in NLRP3 inflammasome domains and Gasdermin D

As previously mentioned, NLRP3 canonical activation includes a priming and an activation step. The priming step, triggered by an activator stimulus mediated by NF-κB, promotes synthesis of NLRP3 domain and pro-IL-1β and controls NLRP3 post-translational modifications[36,49,50,120].

To confirm that $A\beta_{1-42}$ oligomers were able to act as a priming stimulus in acute hippocampal slices we assessed the levels of the inflammasome components by WB (**Fig. 10**). There was a significant increase in NLRP3 protein (1.56 ± 0.16, $p<0.01$), but not in ASC (1.06 ± 0.05, $p>0.05$), in slices incubated with $A\beta_{1-42}$ oligomers. Active Caspase-1, indicative of autoproteolytic cleavage of pro-Caspase-1 and thus of inflammasome activation, also depicted a higher expression in Aβ-incubated slices (1.38 ± 0.03, $p<0.0001$).

As mentioned before, GSDMD, the effector protein in pyroptosis, is cleaved by Caspase-1, releasing the N-terminal domain that migrates to the plasma membrane and initiates cell death by pyroptosis. No differences were detected in full-length GSDMD (1.04 ± 0.01, $p>0.05$) between the two conditions, but the expression of the N-terminal fragment of GSDMD, released by Caspase-1-mediated GSDMD cleavage, was augmented in Aβ-incubated slices (1.41 ± 0.09, $p<0.001$). This result suggests that $A\beta_{1-42}$ oligomers can trigger cell death by pyroptosis in this system.

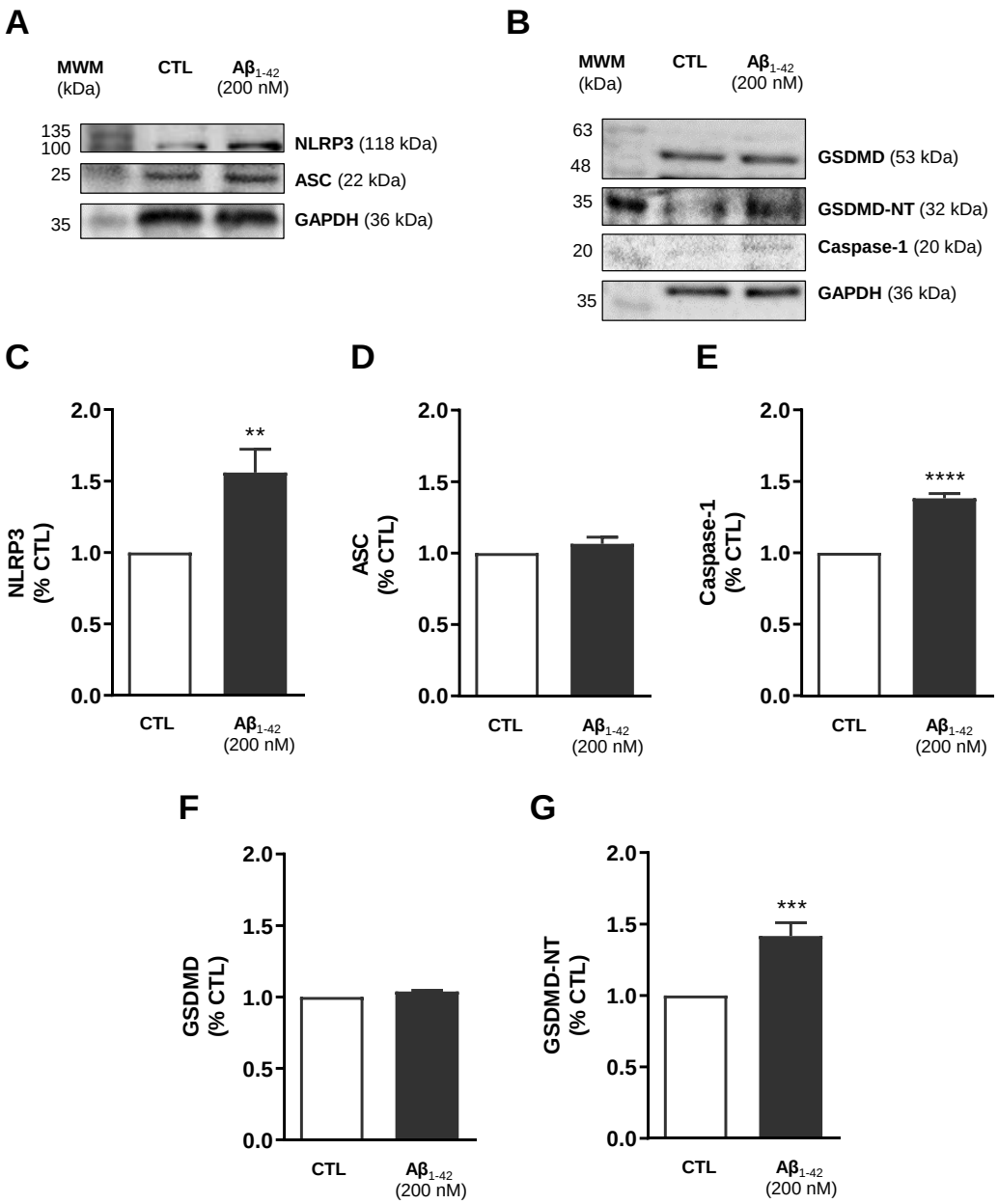

Figure 10. Aβ$_{1-42}$ oligomers induce changes in NLRP3 inflammasome domains and Gasdermin D in hippocampal slices. Representative immunoblots of **(A-B)** NLRP3, ASC, GSDMD, GSDMD-NT, Caspase-1 and GAPDH. Densitometry analysis of **(C)** NLRP3 domain, **(D)** ASC, **(E)** Caspase-1, **(F)** Full-length GSDMD and **(G)** GSDMD-NT was performed with ImageJ software using GAPDH as the loading control. Results are presented as percentage of CTL slices. Increased levels of NLRP3 domain, Caspase-1 and GSDMD-NT were observed in Aβ-incubated slices compared with CTL ones. All values are mean ± SEM. N=7 independent experiments. Statistical tests were performed with *t*-test, **p<0.01, ***p<0.001, ****p<0.0001.

4.1.3. Aβ$_{1-42}$ oligomers trigger IL-1β upregulation

Overproduction of pro-inflammatory cytokines by glial cells, such as IL-1β, is a classical hallmark in AD known to contribute to APP cleavage, leading to Aβ formation and deposition [129].

After proving the occurrence of reactive gliosis in Aβ-incubated slices, as well as increased expression of active Caspase-1 suggestive of NLRP3 inflammasome activation, an ELISA was performed to confirm that the production of IL-1β was indeed exacerbated in slices maintained in the presence of Aβ$_{1-42}$ oligomers, compared to CTL ones.

As can be observed in **Fig. 11**, Aβ$_{1-42}$ oligomers significantly upregulate IL-1β production (137 ± 8.99%, $p<0.01$). It is worthwhile to mention that the antibody used in ELISA does not distinguish between the pro-inflammatory cytokine and its immature form (pro-IL-1β). Since NLRP3 domain was increased in Aβ$_{1-42}$ condition, confirming Aβ-induced priming, an increase in pro-IL-1β was also expected. On the other hand, given the increased expression of active Caspase-1 in slices incubated with Aβ$_{1-42}$ oligomers, we can anticipate a higher processing of pro-IL-1β and thus an increased release of the active cytokine in this condition. To fully prove this, several attempts were made to quantify IL-1β in aCSF, but unfortunately with no success.

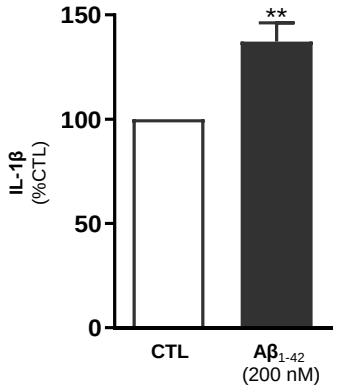

Figure 11. Aβ induces IL-1β upregulation in hippocampal slices. Results are presented as percentage of CTL slices. There was a significant increase of IL-1β expression in Aβ-incubated slices compared with CTL ones. All values are mean ± SEM. N=7 independent experiments. Statistical tests were performed with t-test, **p<0.01.

4.2. Effect of NLRP3 inflammasome inhibitor on $A\beta_{1-42}$ oligomers-induced changes on neuroinflammatory milieu

After validating the model chosen for this work, in terms of the changes induced by $A\beta_{1-42}$ oligomers on several neuroinflammation markers, we addressed the impact of the selective NLRP3 inflammasome inhibitor MCC950 in preventing the observed changes.

Thus, WB and ELISA were performed in hippocampal lysates obtained from slices incubated in aCSF for 5h (CTL group) and incubated with 200nM of $A\beta_{1-42}$ oligomers ($A\beta_{1-42}$ condition) from the second to the fourth hour, in the presence or not of 1 µM MCC950 (MCC950 + $A\beta_{1-42}$ and MCC950 conditions, respectively), as represented in **Fig. 7**.

4.2.1. MCC950 decreases $A\beta_{1-42}$-induced reactive gliosis

We showed that $A\beta_{1-42}$ oligomers induced an increase in astrogliosis, showed by an overexpression of GFAP and C3d, and in microglia activation, confirmed by an increased CD68 expression. In this section we evaluated, through WB, the impact of MCC950 (1µM) on the levels of GFAP and C3d (**Fig. 12**) and on Iba-1 and CD68 (**Fig. 13**).

Fig. 12 shows that MCC950 prevented the Aβ-induced astrogliosis since hippocampal slices incubated with MCC950 present significantly lower levels of GFAP (Aβ: 1.34 ± 0.08 vs MCC+Aβ: 0.89 ± 0.07; $p<0.001$) and of C3d (Aβ: 1.27 ± 0.09 vs MCC950+Aβ: 1.01 ± 0.07; $p<0.05$) than the ones incubated with $A\beta_{1-42}$ oligomers. MCC950 was also able to abolish the increase in CD68 expression induced by $A\beta_{1-42}$ oligomers in hippocampal slices (**Fig. 13**, Aβ: 1.34 ± 0.05 vs MCC950+Aβ: 0.93 ± 0.09; $p<0.001$), while Iba-1 expression remained unchanged by its presence (CTL: 1.16 ± 0.11; Aβ: 1.25 ± 0.07; MCC+Aβ: 1.09 ± 0.15). MCC950 alone had no effect on the expression of GFAP, C3d, Iba-1 and CD68.

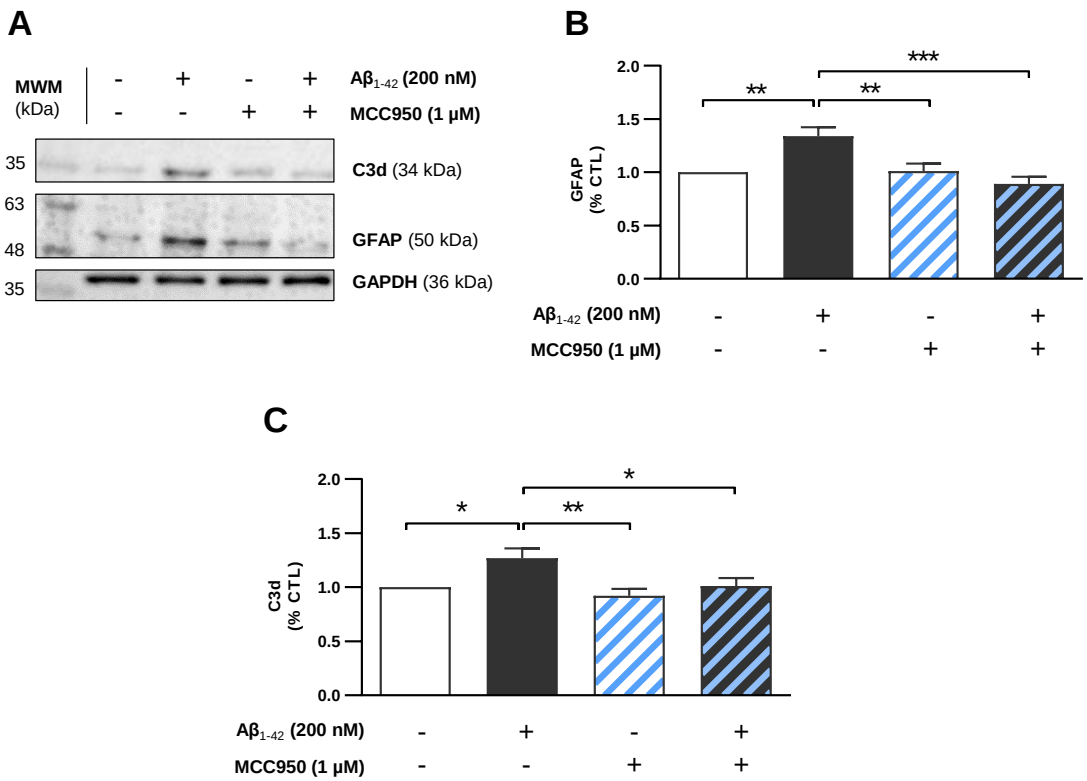

Figure 12. Impact of MCC950 in $A\beta_{1-42}$-induced astrogliosis. (A) Representative immunoblots of GFAP, C3d and GAPDH in CTL slices and in slices incubated with Aβ, MCC950 and both. Densitometry analysis of **(B)** GFAP and **(C)** C3d was performed with ImageJ software using GAPDH as the loading control. Results are presented as percentage of CTL slices. MCC950 prevented the Aβ-induced increase in GFAP and C3d. All values are mean ± SEM. N=7 independent experiments. Statistical tests were performed with one-way ANOVA, followed by Holm-Šídák's multiple comparison test, *p<0.05, **p<0.01, ***p<0.001, as indicated by the lines above the bars.

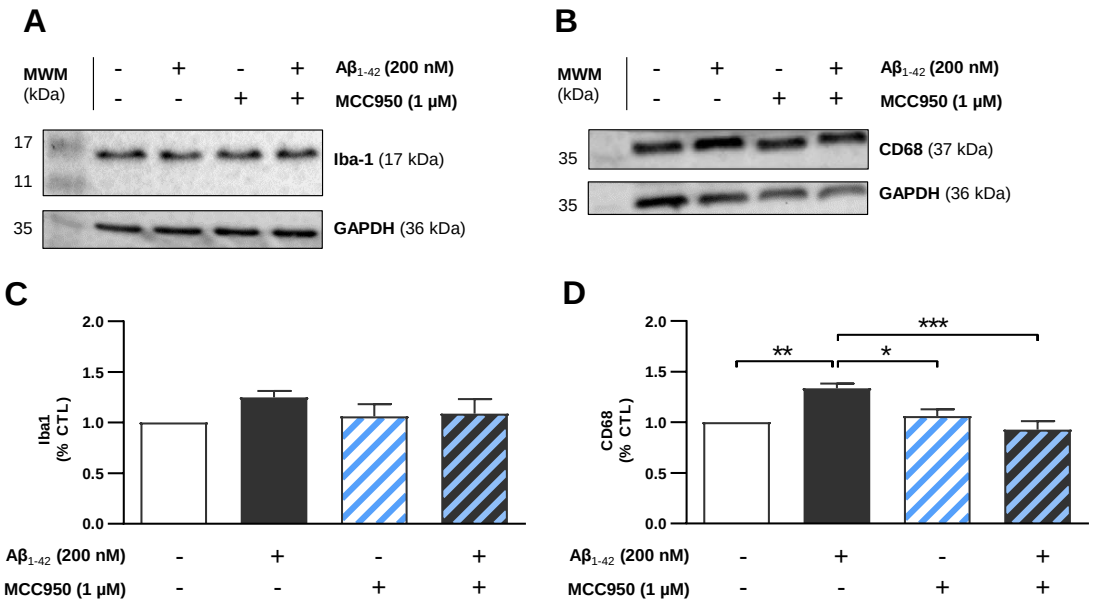

Figure 13. Impact of MCC950 in Aβ$_{1-42}$-induced microglia activation. Representative immunoblots of **(A-B)** Iba-1, CD68 and GAPDH in CTL slices and in slices incubated with Aβ, MCC950 and both. Densitometry analysis of **(C)** Iba-1 and **(D)** CD68 was performed with ImageJ software using GAPDH as the loading control. Results are presented as percentage of CTL slices. MCC950 prevented the Aβ-induced increase in CD68. All values are mean ± SEM. N=7 independent experiments. Statistical tests were performed with one-way ANOVA, followed by Holm-Šídák's multiple comparison test, *p<0.05, **p<0.01, ***p<0.001, as indicated by the lines above the bars.

4.2.2. MCC950 prevents the Aβ$_{1-42}$-induced changes in NLRP3 inflammasome domains and in Gasdermin D cleavage

Significant increases of NLRP3 protein, Caspase-1 and GSDMD-NT were observed in hippocampal slices incubated with Aβ$_{1-42}$ oligomers, as compared with CTL slices. Here, we address, through WB, the impact of MCC950 (1μM) on these alterations.

As depicted in **Fig. 14**, MCC950 prevented the increase in the levels of Caspase-1 (Aβ: 1.37 ± 0.05 vs MCC950+Aβ: 0.98 ± 0.09; p<0.001) but did not alter the expression of the NLRP3 domain induced by Aβ$_{1-42}$ oligomers (Aβ: 1.32 ± 0.06 vs MCC950+Aβ: 1.26 ± 0.11; p>0.05). The expression of ASC domain, unchanged by Aβ$_{1-42}$ oligomers, was not influenced by the presence of MCC950 (Aβ: 1.18 ± 0.08 vs MCC950+Aβ: 1.00 ± 0.11, p>0.05). These results indicate

that MCC950 impairs NLRP3 inflammasome activation, while having no effect in the priming step.

Regarding the impact of MCC950 on cell death through pyroptosis, evaluated by the formation of the GSDMD-NT, **Fig. 15** indicates that MCC950 had no effect on the expression of FL-GSDMD (Aβ: 1.08 ± 0.07 vs MCC950+Aβ: 1.04 ± 0.03, $p>0.05$), but avoided the Aβ-induced increase in GSDMD-NT formation (Aβ: 1.44 ± 0.06 vs MCC950+Aβ: 1.15 ± 0.07; $p<0.01$). These results indicate that MCC950 halts the occurrence of Aβ-induced cell death by pyroptosis in this system.

Moreover, MCC950 alone had no effect on the expression of the proteins evaluated in **Fig. 14** and **15**, since their levels in hippocampal slices incubated with MCC950 alone were not statistically different from CTL slices.

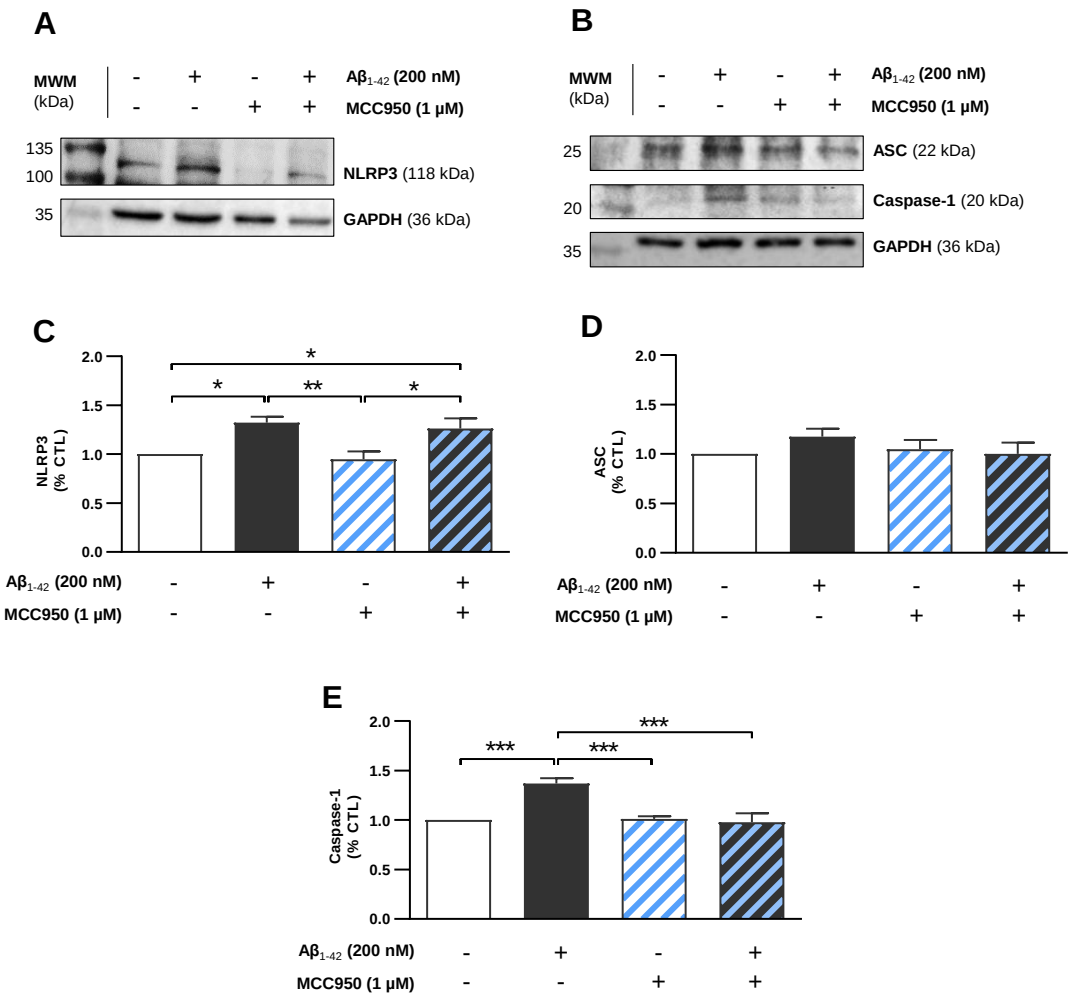

Figure 14. Impact of MCC950 in Aβ$_{1-42}$-induced changes in NLRP3 inflammasome components. (A-B) Representative immunoblots of NLRP3, ASC, Caspase-1 and GAPDH in CTL slices and in slices incubated with Aβ, MCC950 and both. Densitometry analysis of **C)** NLRP3 domain, **D)** ASC and **E)** Caspase-1 was performed with ImageJ software using GAPDH as the loading control. Results are presented as percentage of CTL slices. MCC950 prevented the Aβ-induced increase in Caspase-1. All values are mean ± SEM. N=6-7 independent experiments. Statistical tests were performed with one-way ANOVA, followed by Holm-Šídák's multiple comparison test, *p<0.05, **p<0.01, ***p<0.001, as indicated by the lines above the bars.

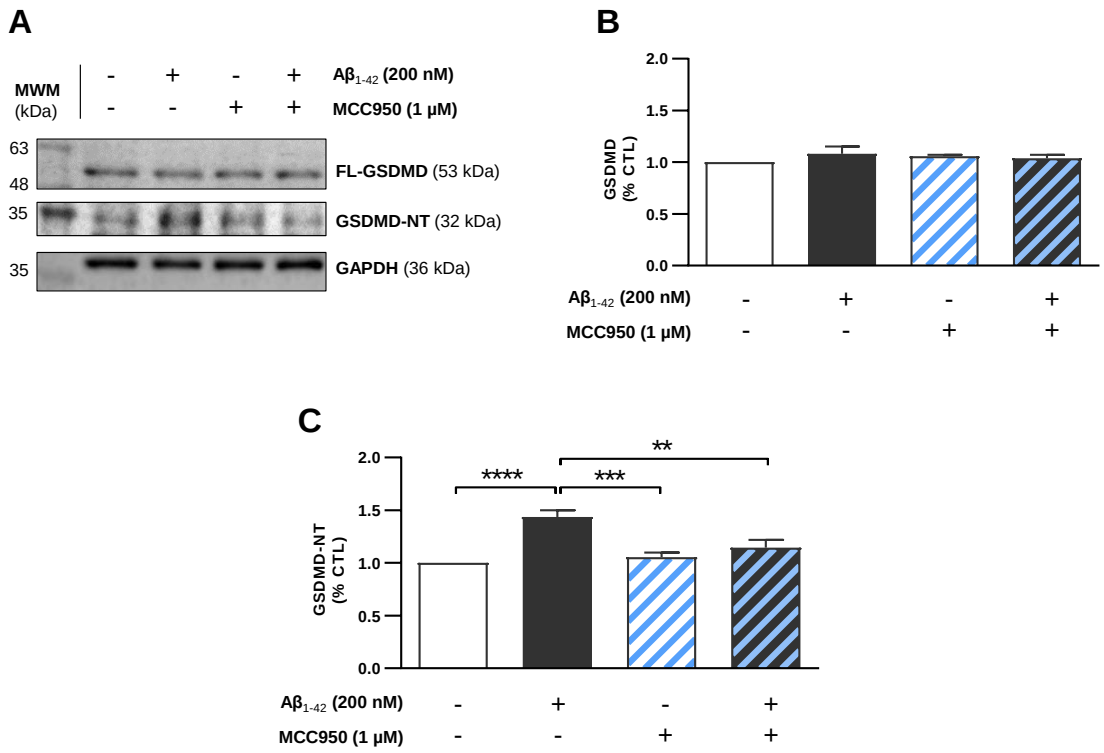

Figure 15. Impact of MCC950 in Aβ$_{1-42}$-induced cleavage of Gasdermin D. (A) Representative immunoblots of FL-GSDMD, GSDMD-NT and GAPDH in CTL slices and in slices incubated with Aβ, MCC950 and both. Densitometry analysis of **(B)** GSDMD and **(C)** GSDMD-NT was performed with ImageJ software using GAPDH as the loading control. Results are presented as percentage of CTL slices. MCC950 prevented the Aβ-induced increase in GSDMD-NT formation. All values are mean ± SEM. N=7 independent experiments. Statistical tests were performed with one-way ANOVA, followed by Holm-Šídák's multiple comparison test, **p<0.01, ***p<0.001, ****p<0.0001, as indicated by the lines above the bars.

4.2.3. MCC950 does not impact Aβ$_{1-42}$-induced IL-1β upregulation

As the literature states[130], MCC950 binds specifically to the NLRP3 protein of the inflammasome hindering its oligomerization and activation, and subsequently impairing Caspase-1-mediated IL-1β maturation.

The Aβ-induced increase in NLRP3 domain and in pro-IL-1β / IL-1β suggested that Aβ$_{1-42}$ oligomers trigger the priming step of the canonical NLRP3 pathway. Corroborating the literature, MCC950 did not influence the Aβ-increase in the NLRP3 domain. Likewise, as depicted in **Fig. 16**, MCC950 does not affect

the upregulation of pro-IL-1β / IL-1β in hippocampal slices incubated with the $A\beta_{1-42}$ oligomers (Aβ: 132 ± 5.79% vs MCC950+Aβ: 130 ± 6.65%; p>0.05).

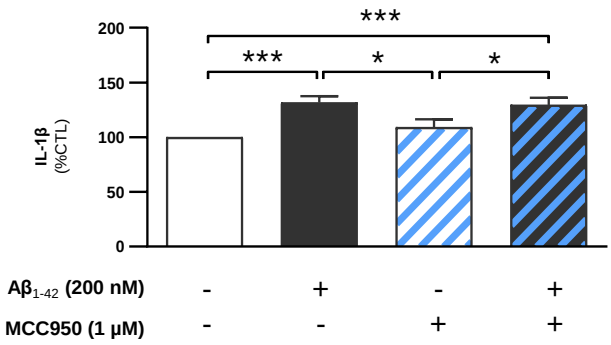

Figure 16. Impact of MCC950 in $A\beta_{1-42}$-induced upregulation of IL-1β levels. Results are presented as percentage to CTL. MCC950 does not prevent the Aβ-induced increase in pro-IL-1β / IL-1β levels. All values are mean ± SEM. N=6-8 independent experiments. Statistical tests were performed with one-way ANOVA, followed by Holm-Šídák's multiple comparison test, *p<0.05, ***p<0.001, as indicated by the lines above the bars.

The Aβ-induced increase in Caspase-1 was prevented by MCC950, thus impairing pro-IL-1β processing. To fully prove that pro-IL-1β was not processed in the presence of MCC950, several attempts were made to quantify IL-1β released in all conditions, but unfortunately with no success.

5. Discussion

In this work, the main findings were:

i. Acute hippocampal slices incubated with $A\beta_{1-42}$ revealed increased reactive gliosis and increased NLRP3 inflammasome priming and activation;
ii. The specific NLRP3 inflammasome inhibitor, MCC950, halted $A\beta_{1-42}$-induced reactive gliosis in hippocampal slices, as well as impaired NLRP3 inflammasome priming and activation, subsequently preventing cellular death by pyroptosis.

The model of Aβ-induced toxicity in acute slices was successfully established. At first, we started by using a vibratome to obtain the hippocampal slices, as this machine deals less mechanical damage to the tissue, being more suitable for immunohistochemistry analysis. However, the cutting process in a vibratome requires an edge of the hippocampus to be glued to a support, which makes that section of the tissue inviable, thus yielding less slices (6-8 slices per hippocampus) than a tissue chopper (10-12 slices per hippocampus). The chopper is a viable alternative since it is the gold standard used for electrophysiological recordings, as slices have their cellular integrity mainly preserved[131,132]. To note that as the superficial layers of the slices are more damaged due to the mechanical cut induced by the chopper, these layers were removed in the cryostat and the remaining tissue was then cut into smaller 20 µm sections that were subsequently used in the IHC assays.

The Aβ-induced neuroinflammatory milieu was also successfully characterized. Since $A\beta_{1-42}$ oligomers are described to cause gliosis, we started by determining whether the experimental conditions used were able to reproduce that impact.

Under reactive gliosis both astrocytic markers GFAP and C3d are known to be upregulated in reactive A1 astrocytes[89,91,115,133], thus they were expected to be augmented in the presence of $A\beta_{1-42}$ oligomers. Indeed, our results (**Fig. 8**) confirmed this, revealing a significant increase of both markers in the presence of $A\beta_{1-42}$. GFAP is an intermediate filament that forms a network to provide support and control cellular shape, movement, and function, is known to be

overexpressed in reactive astrocytes due to the increased number and thickness of cellular processes[115,134]. Researchers suggested that exposure to Aβ, as well as activation of NLRP3 inflammasome and subsequent production of inflammatory cytokines in microglia, induce astrocytes conversion to neurotoxic A1 phenotype through the NF-κB pathway[135,136]. It is also known that A1 astrocytes decrease the synaptic density and impair synaptic function through the release of C3, which in turn has been identified as an astroglial-specific NF-κB target that is both necessary and sufficient to produce neuronal impairment through C3aR and intraneuronal calcium signaling[136]. In addition, after C3d was found accumulating around neurons, it is hypothesized that this complement product might be implicated in neuronal damage[135].

Microglia activation was addressed via Iba-1 and CD68. The first one is involved in microglia motility, phagocytosis and cell activation, being expressed in both resting and reactive microglia[116], hence it was expected to be increased, since microglia activation also implies microglia proliferation. However, although a tendency to increased Iba-1 expression was observed in Aβ-incubated slices that was not statistically significant. CD68 is a protein located in lysosomal membranes of M1 and M2 microglia, being especially upregulated in actively phagocytic cells[117,118,137,138]. The results (**Fig. 9**) met the expectations, as CD68 was increased in the presence of $A\beta_{1-42}$, meaning that in this model, the system responded to Aβ oligomers by increasing microglial activation[76-78]. In the future, it should be evaluated whether the increased activated microglia displays the more neurotoxic M1 phenotype, by using M1specific markers, as CD80[139,140], or the more neuroprotective M2 phenotype, by using M2 specific markers, such as YM1[141].

Data (**Fig. 10**) also indicates that $A\beta_{1-42}$ oligomers increased the expression of the inflammasome components NLRP3 protein and active Caspase-1, with the consequent increased formation of the pore-forming GSDMD-NT. Toxic Aβ oligomers are known to act as a priming stimulus, inducing the expression of NLRP3 and pro-IL-1β, through activation of the NF-κB pathway[142,143]. They also serve as an activation stimulus for NLRP3 inflammasome, and in this context this can be proven, as the expression of the p20 subunit of Caspase-1 was

significantly increased in the Aβ, meaning that pro-Caspase-1 was actively cleaved into Caspase-1.

An increase in the proinflammatory cytokine IL-1β production was also observed in hippocampal slices incubated with Aβ oligomers (**Fig. 11**). However, as the ELISA was performed in hippocampal tissue and given that the antibodies used does not distinguish between pro-IL-1β and IL-1β, it was not possible to identify which form was increased. The fact that the levels of active Caspase-1 are increased suggests that, indeed, IL-1β processing and release is also occurring[36,41,43]. Additionally, the increase in the expression of GSDMD-NT (**Fig. 10**) can also be explained by increased Caspase-1 activity, supporting the idea that cell death by pyroptosis is taking place in this system[99,100]. The fact that full-length GSDMD was not decreased as a consequence of its cleavage, might be due to compensatory mechanisms that allow the basal levels of the protein to be maintained. Given the results presented, we concluded that NLRP3 inflammasome priming and activation steps were successfully induced in this model[56].

As previously mentioned, the second half of the work consisted in evaluating the impact of MCC950 in preventing $A\beta_{1-42}$-induced alterations. Indeed, similarly to another study[135], our WB results (**Fig. 12**) indicate that in the presence of MCC950 there were no significant increase in GFAP and C3d expression levels. With NLRP3 inhibited there is less production of pro-inflammatory cytokines and consequently less activation of the NF-κB pathway in astrocytes responsible for the conversion to the neurotoxic A1 phenotype[135,136,143]. MCC950 also hampered microgliosis. WB data (**Fig. 13**) revealed that, in the presence of MCC950, there was a significant decrease in the reactive microglia marker CD68, consequence of the effective inhibition of NLRP3 inflammasome activation in microglia [37].

The literature suggests that MCC950 specifically inhibits NLRP3-inflamassome oligomerisation but does not influence its priming phase[64]. As previously mentioned, toxic Aβ oligomers can act as a priming and activation stimulus, with the first one increasing the expression of NLRP3 and pro-IL-1β, through the NF-κB pathway[142,143]. Indeed, our results (**Fig. 14**) revealed that NLRP3 protein levels were augmented in both Aβ and MCC950+Aβ, meaning that $A\beta_{1-42}$ can still induce NF-κB pathway-mediated increase of NLRP3 protein

and pro-IL-1β / IL-1β expression (**Fig. 16**) independently of MCC950 action. ASC levels remained unchanged as MCC950 does not affect its expression[64].

In the presence of MCC950, active Caspase-1 levels were expectedly lower because of the inhibition of the activation of the inflammasome, which impeded the conversion of pro-Caspase-1 into mature Caspase-1. Likewise, GSDMD-NT levels decreased, as full-length GSDMD was not being actively cleaved by Caspase-1 (**Fig. 15**).

As WB is a semi-quantitative technique, it does not provide information regarding the morphology of glial cells, which is also important to evaluate reactive gliosis and the impact of MCC950 upon this event. Therefore, to complement the information given by WB an IHC analysis was endeavoured. To visualize the impact of MCC950 upon the $A\beta_{1-42}$-induced reactive astrogliosis a double staining of GFAP and C3d was attempted, while a double staining of Iba-1 and CD68 was struggled to address the microglia activation phenotypes promoted by $A\beta_{1-42}$ oligomers and the impact of MCC950 upon them. Moreover, since WB showed that MCC950 was able to decrease the levels of GSDMD N-terminal fragment, pointing to a decrease in cell death by pyroptosis, we tried to evaluate the occurrence of Aβ-induced neuronal death by pyroptosis and the impact of MCC950 upon this event, with a double staining of the neuronal nuclei marker (NeuN) and GSDMD. Unfortunately, confocal images had a lot of unspecific binding and no clear images could be obtained, indicating that further optimizations, that could not be achieved in the time span of the present work, are still required.

In summary, independently of the lack of results that would be given by the IHC assays, it became clear that MCC950 has the potential to be used as a neuroprotective molecule against $A\beta_{1-42}$-induced reactive gliosis and pyroptotic cell death, through inhibition of the NLRP3 inflammasome.

Future studies should focus on developing structure-guided direct inhibitors[62], possibly combining them with MCC950, so that new therapeutical approaches can be explored. Also, further research is required to better understand the pyroptosis phenomenon, specifically, the biology of pore formation in the cell membrane and respective lipid-binding properties[144].

6. Conclusion and Future Perspectives

In the present work, selective NLRP3 inhibitor MCC950 was studied in a model of Aβ-induced toxicity in acute hippocampus slices, regarding its ability to mitigate the neuroinflammatory response and cell death by pyroptosis promoted by $A\beta_{1-42}$ oligomers. Overall, the findings suggest that the model was successfully validated as $A\beta_{1-42}$ oligomers triggered gliosis and activated pyroptotic agents. Moreover, MCC950 could prevent such noxious effects, further supporting its role as a neuroprotective molecule and reinforcing its potential as a drug candidate for the preventive treatment of AD.

The current understanding of AD pathogenesis indicates that investments in prevention and early intervention in AD are an ever-growing need. However, this perspective faces many challenges, such as how to identify patients that are more susceptible to develop the disease and how to monitor the effects of a given intervention as the disease progresses[145]. Recent scientific breakthroughs have been made regarding the development of promising non-invasive techniques for *in vivo* detection of Aβ deposits, which allow the disease to be detected much before it starts to manifest[146]. In this context, preventive administration of MCC950 could be decisive to impede the neuroinflammatory-derived cellular loss, consequently avoiding the appearance of symptoms.

Currently, the idea of a single drug to prevent/treat AD is considered utopic. As the knowledge about the disease increases, more do researchers realize that AD is indeed a consequence of a complex cascade of events with many networks of interactions. For this reason, it is likely that a future pharmacological approach arises from the combination of different drugs that target crucial checkpoints in the development of the disease[39].

7. References

1 Benarde, M. A. *Our Precarious Habitat*. (Norton, 1970).

2 Shepherd, A. *et al.* Evaluation of attention in APP/PS1 mice shows impulsive and compulsive behaviours. *Genes, brain, and behavior*, doi:10.1111/gbb.12594 (2019).

3 Masters, C. L. *et al.* Alzheimer's disease. *Nature reviews. Disease primers* **1**, 15056, doi:10.1038/nrdp.2015.56 (2015).

4 Gonzalez-Reyes, R. E., Nava-Mesa, M. O., Vargas-Sanchez, K., Ariza-Salamanca, D. & Mora-Munoz, L. Involvement of Astrocytes in Alzheimer's Disease from a Neuroinflammatory and Oxidative Stress Perspective. *Frontiers in molecular neuroscience* **10**, 427, doi:10.3389/fnmol.2017.00427 (2017).

5 Selkoe, D. J. The molecular pathology of Alzheimer's disease. *Neuron* **6**, 487-498, doi:10.1016/0896-6273(91)90052-2 (1991).

6 Hardy, J. & Selkoe, D. J. The amyloid hypothesis of Alzheimer's disease: progress and problems on the road to therapeutics. *Science (New York, N.Y.)* **297**, 353-356, doi:10.1126/science.1072994 (2002).

7 El-Hayek, Y. H. *et al.* Tip of the Iceberg: Assessing the Global Socioeconomic Costs of Alzheimer's Disease and Related Dementias and Strategic Implications for Stakeholders. *Journal of Alzheimer's Disease* **70**, 323-341, doi:10.3233/JAD-190426 (2019).

8 Castro, D. M., Dillon, C., Machnicki, G. & Allegri, R. F. The economic cost of Alzheimer's disease: Family or public health burden? *Dement Neuropsychol* **4**, 262-267, doi:10.1590/s1980-57642010dn40400003 (2010).

9 Wimo, A. *et al.* The worldwide costs of dementia 2015 and comparisons with 2010. *Alzheimer's & dementia : the journal of the Alzheimer's Association* **13**, 1-7, doi:10.1016/j.jalz.2016.07.150 (2017).

10 Wang, J., Gu, B. J., Masters, C. L. & Wang, Y.-J. A systemic view of Alzheimer disease — insights from amyloid-β metabolism beyond the brain. *Nature Reviews Neurology* **13**, 612, doi:10.1038/nrneurol.2017.111 (2017).

11 Herrup, K. The case for rejecting the amyloid cascade hypothesis. *Nature neuroscience* **18**, 794-799, doi:10.1038/nn.4017 (2015).

12 Alzheimer, A., Stelzmann, R. A., Schnitzlein, H. N. & Murtagh, F. R. An English translation of Alzheimer's 1907 paper, "Uber eine eigenartige Erkankung der Hirnrinde". *Clinical anatomy (New York, N.Y.)* **8**, 429-431, doi:10.1002/ca.980080612 (1995).

13 Weickenmeier, J., Kuhl, E. & Goriely, A. Multiphysics of Prionlike Diseases: Progression and Atrophy. *Physical Review Letters* **121**, 158101, doi:10.1103/PhysRevLett.121.158101 (2018).

14 Zhou, Y., Sun, Y., Ma, Q. H. & Liu, Y. Alzheimer's disease: amyloid-based pathogenesis and potential therapies. *Cell stress* **2**, 150-161, doi:10.15698/cst2018.07.143 (2018).

15 Hernandez Zimbron, L. & Rivas-Arancibia, S. Deciphering an interplay of proteins associated with amyloid β 1-42 peptide and molecular mechanisms of Alzheimer's disease. *Reviews in the neurosciences* **25**, doi:10.1515/revneuro-2014-0025 (2014).

16 Heneka, M. T., Golenbock, D. T. & Latz, E. Innate immunity in Alzheimer's disease. *Nat Immunol* **16**, 229-236, doi:10.1038/ni.3102 (2015).

17 Mucke, L. & Selkoe, D. J. Neurotoxicity of amyloid beta-protein: synaptic and network dysfunction. *Cold Spring Harbor perspectives in medicine* **2**, a006338, doi:10.1101/cshperspect.a006338 (2012).

18 Luciunaite, A. *et al.* Soluble Abeta oligomers and protofibrils induce NLRP3 inflammasome activation in microglia. *J Neurochem*, e14945, doi:10.1111/jnc.14945 (2019).

19 Golde, T. E., Eckman, C. B. & Younkin, S. G. Biochemical detection of Aβ isoforms: implications for pathogenesis, diagnosis, and treatment of Alzheimer's disease.

Biochimica et Biophysica Acta (BBA) - Molecular Basis of Disease **1502**, 172-187, doi:https://doi.org/10.1016/S0925-4439(00)00043-0 (2000).

20 Ransohoff, R. M. How neuroinflammation contributes to neurodegeneration. *Science (New York, N.Y.)* **353**, 777-783, doi:10.1126/science.aag2590 (2016).

21 Bartsch, T. & Wulff, P. The hippocampus in aging and disease: From plasticity to vulnerability. *Neuroscience* **309**, 1-16, doi:10.1016/j.neuroscience.2015.07.084 (2015).

22 Smith, C. J. *et al.* Investigations on alterations of hippocampal circuit function following mild traumatic brain injury. *Journal of visualized experiments : JoVE*, e4411-e4411, doi:10.3791/4411 (2012).

23 *The Hippocampus Book*. (Oxford University Press, 2006).

24 Jacob, H. J. & Kwitek, A. E. Rat genetics: attaching physiology and pharmacology to the genome. *Nature reviews. Genetics* **3**, 33-42, doi:10.1038/nrg702 (2002).

25 Heneka, M. T. *et al.* Neuroinflammation in Alzheimer's disease. *The Lancet. Neurology* **14**, 388-405, doi:10.1016/s1474-4422(15)70016-5 (2015).

26 DiSabato, D. J., Quan, N. & Godbout, J. P. Neuroinflammation: the devil is in the details. *J Neurochem* **139 Suppl 2**, 136-153, doi:10.1111/jnc.13607 (2016).

27 Rathinam, V. A., Vanaja, S. K. & Fitzgerald, K. A. Regulation of inflammasome signaling. *Nat Immunol* **13**, 333-342, doi:10.1038/ni.2237 (2012).

28 Leyns, C. E. G. & Holtzman, D. M. Glial contributions to neurodegeneration in tauopathies. *Mol Neurodegener* **12**, 50-50, doi:10.1186/s13024-017-0192-x (2017).

29 Guerreiro, R. *et al.* TREM2 variants in Alzheimer's disease. *The New England journal of medicine* **368**, 117-127, doi:10.1056/NEJMoa1211851 (2013).

30 Castellano, J. M. *et al.* Human apoE isoforms differentially regulate brain amyloid-beta peptide clearance. *Science translational medicine* **3**, 89ra57, doi:10.1126/scitranslmed.3002156 (2011).

31 Huang, Y. & Mahley, R. W. Apolipoprotein E: structure and function in lipid metabolism, neurobiology, and Alzheimer's diseases. *Neurobiology of disease* **72 Pt A**, 3-12, doi:10.1016/j.nbd.2014.08.025 (2014).

32 Corder, E. H. *et al.* Gene dose of apolipoprotein E type 4 allele and the risk of Alzheimer's disease in late onset families. *Science (New York, N.Y.)* **261**, 921-923, doi:10.1126/science.8346443 (1993).

33 McKee, A. C. *et al.* The first NINDS/NIBIB consensus meeting to define neuropathological criteria for the diagnosis of chronic traumatic encephalopathy. *Acta neuropathologica* **131**, 75-86, doi:10.1007/s00401-015-1515-z (2016).

34 Lozano, D. *et al.* Neuroinflammatory responses to traumatic brain injury: etiology, clinical consequences, and therapeutic opportunities. *Neuropsychiatric disease and treatment* **11**, 97-106, doi:10.2147/ndt.S65815 (2015).

35 Cherry, J. D. *et al.* Microglial neuroinflammation contributes to tau accumulation in chronic traumatic encephalopathy. *Acta neuropathologica communications* **4**, 112, doi:10.1186/s40478-016-0382-8 (2016).

36 Yang, Y., Wang, H., Kouadir, M., Song, H. & Shi, F. Recent advances in the mechanisms of NLRP3 inflammasome activation and its inhibitors. *Cell Death & Disease* **10**, 128, doi:10.1038/s41419-019-1413-8 (2019).

37 Dempsey, C. *et al.* Inhibiting the NLRP3 inflammasome with MCC950 promotes non-phlogistic clearance of amyloid-β and cognitive function in APP/PS1 mice. *Brain, behavior, and immunity* **61**, 306-316 (2016).

38 Heneka, M. T. *et al.* NLRP3 is activated in Alzheimer's disease and contributes to pathology in APP/PS1 mice. *Nature* **493**, 674-678, doi:10.1038/nature11729 (2013).

39 Daniels, M. J. D. *et al.* Fenamate NSAIDs inhibit the NLRP3 inflammasome and protect against Alzheimer's disease in rodent models. *Nature Communications* **7**, 12504, doi:10.1038/ncomms12504 (2016).

40 Thawkar, B. S. & Kaur, G. Inhibitors of NF-κB and P2X7/NLRP3/Caspase 1 pathway in microglia: Novel therapeutic opportunities in neuroinflammation induced early-stage Alzheimer's disease. *Journal of neuroimmunology* **326**, 62-74, doi:10.1016/j.jneuroim.2018.11.010 (2019).
41 Stutz, A., Golenbock, D. T. & Latz, E. Inflammasomes: too big to miss. *The Journal of clinical investigation* **119**, 3502-3511, doi:10.1172/JCI40599 (2009).
42 Srinivasula, S. M. *et al.* The PYRIN-CARD protein ASC is an activating adaptor for caspase-1. *The Journal of biological chemistry* **277**, 21119-21122, doi:10.1074/jbc.C200179200 (2002).
43 Liepinsh, E. *et al.* The death-domain fold of the ASC PYRIN domain, presenting a basis for PYRIN/PYRIN recognition. *Journal of molecular biology* **332**, 1155-1163, doi:10.1016/j.jmb.2003.07.007 (2003).
44 Murphy, N., Grehan, B. & Lynch, M. A. Glial uptake of amyloid beta induces NLRP3 inflammasome formation via cathepsin-dependent degradation of NLRP10. *Neuromolecular medicine* **16**, 205-215, doi:10.1007/s12017-013-8274-6 (2014).
45 He, Y., Hara, H. & Núñez, G. Mechanism and Regulation of NLRP3 Inflammasome Activation. *Trends in biochemical sciences* **41**, 1012-1021, doi:10.1016/j.tibs.2016.09.002 (2016).
46 He, Y., Zeng, M. Y., Yang, D., Motro, B. & Núñez, G. NEK7 is an essential mediator of NLRP3 activation downstream of potassium efflux. *Nature* **530**, 354-357, doi:10.1038/nature16959 (2016).
47 Yan, Y. *et al.* Dopamine controls systemic inflammation through inhibition of NLRP3 inflammasome. *Cell* **160**, 62-73, doi:10.1016/j.cell.2014.11.047 (2015).
48 Voet, S., Srinivasan, S., Lamkanfi, M. & van Loo, G. Inflammasomes in neuroinflammatory and neurodegenerative diseases. *EMBO molecular medicine* **11**, doi:10.15252/emmm.201810248 (2019).
49 Yang, J., Liu, Z. & Xiao, T. S. Post-translational regulation of inflammasomes. *Cellular & Molecular Immunology* **14**, 65-79, doi:10.1038/cmi.2016.29 (2017).
50 Juliana, C. *et al.* Non-transcriptional priming and deubiquitination regulate NLRP3 inflammasome activation. *The Journal of biological chemistry* **287**, 36617-36622, doi:10.1074/jbc.M112.407130 (2012).
51 Mémet, S. NF-kappaB functions in the nervous system: from development to disease. *Biochemical pharmacology* **72**, 1180-1195, doi:10.1016/j.bcp.2006.09.003 (2006).
52 Bauernfeind, F. G. *et al.* Cutting edge: NF-kappaB activating pattern recognition and cytokine receptors license NLRP3 inflammasome activation by regulating NLRP3 expression. *Journal of immunology (Baltimore, Md. : 1950)* **183**, 787-791, doi:10.4049/jimmunol.0901363 (2009).
53 Pellegrini, C., Antonioli, L., Lopez-Castejon, G., Blandizzi, C. & Fornai, M. Canonical and Non-Canonical Activation of NLRP3 Inflammasome at the Crossroad between Immune Tolerance and Intestinal Inflammation. *Frontiers in immunology* **8**, 36, doi:10.3389/fimmu.2017.00036 (2017).
54 Vanaja, S. K., Rathinam, V. A. & Fitzgerald, K. A. Mechanisms of inflammasome activation: recent advances and novel insights. *Trends in cell biology* **25**, 308-315, doi:10.1016/j.tcb.2014.12.009 (2015).
55 Blum-Degen, D. *et al.* Interleukin-1 beta and interleukin-6 are elevated in the cerebrospinal fluid of Alzheimer's and de novo Parkinson's disease patients. *Neuroscience letters* **202**, 17-20, doi:10.1016/0304-3940(95)12192-7 (1995).
56 Sheedy, F. J. *et al.* CD36 coordinates NLRP3 inflammasome activation by facilitating intracellular nucleation of soluble ligands into particulate ligands in sterile inflammation. *Nat Immunol* **14**, 812-820, doi:10.1038/ni.2639 (2013).

57 Kahlenberg, J. M. & Dubyak, G. R. Mechanisms of caspase-1 activation by P2X7 receptor-mediated K+ release. *American journal of physiology. Cell physiology* **286**, C1100-1108, doi:10.1152/ajpcell.00494.2003 (2004).
58 Griffin, W. S., Liu, L., Li, Y., Mrak, R. E. & Barger, S. W. Interleukin-1 mediates Alzheimer and Lewy body pathologies. *J Neuroinflammation* **3**, 5, doi:10.1186/1742-2094-3-5 (2006).
59 Pickering, M. & O'Connor, J. J. Pro-inflammatory cytokines and their effects in the dentate gyrus. *Progress in brain research* **163**, 339-354, doi:10.1016/s0079-6123(07)63020-9 (2007).
60 Tan, M. S. *et al.* NLRP3 polymorphisms are associated with late-onset Alzheimer's disease in Han Chinese. *Journal of neuroimmunology* **265**, 91-95, doi:10.1016/j.jneuroim.2013.10.002 (2013).
61 El-Sharkawy, L. Y., Brough, D. & Freeman, S. Inhibiting the NLRP3 Inflammasome. *Molecules (Basel, Switzerland)* **25**, doi:10.3390/molecules25235533 (2020).
62 Zahid, A., Li, B., Kombe, A. J. K., Jin, T. & Tao, J. Pharmacological Inhibitors of the NLRP3 Inflammasome. **10**, doi:10.3389/fimmu.2019.02538 (2019).
63 Coll, R. C. *et al.* MCC950 directly targets the NLRP3 ATP-hydrolysis motif for inflammasome inhibition. *Nature chemical biology* **15**, 556-559, doi:10.1038/s41589-019-0277-7 (2019).
64 Coll, R. C. *et al.* A small-molecule inhibitor of the NLRP3 inflammasome for the treatment of inflammatory diseases. *Nat Med* **21**, 248-255, doi:10.1038/nm.3806 (2015).
65 Daneman, R. & Prat, A. The blood-brain barrier. *Cold Spring Harbor perspectives in biology* **7**, a020412, doi:10.1101/cshperspect.a020412 (2015).
66 Dong, Y. & Benveniste, E. N. Immune function of astrocytes. *Glia* **36**, 180-190, doi:10.1002/glia.1107 (2001).
67 Guo, H., Callaway, J. B. & Ting, J. P. Inflammasomes: mechanism of action, role in disease, and therapeutics. *Nat Med* **21**, 677-687, doi:10.1038/nm.3893 (2015).
68 Schroder, K. & Tschopp, J. The Inflammasomes. *Cell* **140**, 821-832, doi:https://doi.org/10.1016/j.cell.2010.01.040 (2010).
69 Liddelow, S. A. & Barres, B. A. Reactive Astrocytes: Production, Function, and Therapeutic Potential. *Immunity* **46**, 957-967, doi:10.1016/j.immuni.2017.06.006 (2017).
70 Lucin, K. M. & Wyss-Coray, T. Immune activation in brain aging and neurodegeneration: too much or too little? *Neuron* **64**, 110-122, doi:10.1016/j.neuron.2009.08.039 (2009).
71 Griffin, W. S. *et al.* Glial-neuronal interactions in Alzheimer's disease: the potential role of a 'cytokine cycle' in disease progression. *Brain pathology (Zurich, Switzerland)* **8**, 65-72, doi:10.1111/j.1750-3639.1998.tb00136.x (1998).
72 Kettenmann, H., Hanisch, U. K., Noda, M. & Verkhratsky, A. Physiology of microglia. *Physiological reviews* **91**, 461-553, doi:10.1152/physrev.00011.2010 (2011).
73 Rock, R. B. *et al.* Role of microglia in central nervous system infections. *Clinical microbiology reviews* **17**, 942-964, table of contents, doi:10.1128/cmr.17.4.942-964.2004 (2004).
74 Gold, M. & El Khoury, J. beta-amyloid, microglia, and the inflammasome in Alzheimer's disease. *Seminars in immunopathology* **37**, 607-611, doi:10.1007/s00281-015-0518-0 (2015).
75 Wang, W. Y., Tan, M. S., Yu, J. T. & Tan, L. Role of pro-inflammatory cytokines released from microglia in Alzheimer's disease. *Annals of translational medicine* **3**, 136, doi:10.3978/j.issn.2305-5839.2015.03.49 (2015).
76 Asai, H. *et al.* Depletion of microglia and inhibition of exosome synthesis halt tau propagation. *Nature neuroscience* **18**, 1584-1593, doi:10.1038/nn.4132 (2015).

77 Wu, J. W. *et al.* Small misfolded Tau species are internalized via bulk endocytosis and anterogradely and retrogradely transported in neurons. *The Journal of biological chemistry* **288**, 1856-1870, doi:10.1074/jbc.M112.394528 (2013).
78 Bolos, M. *et al.* Direct Evidence of Internalization of Tau by Microglia In Vitro and In Vivo. *Journal of Alzheimer's disease : JAD* **50**, 77-87, doi:10.3233/jad-150704 (2016).
79 Halle, A. *et al.* The NALP3 inflammasome is involved in the innate immune response to amyloid-beta. *Nat Immunol* **9**, 857-865, doi:10.1038/ni.1636 (2008).
80 Frackowiak, J. *et al.* Ultrastructure of the microglia that phagocytose amyloid and the microglia that produce beta-amyloid fibrils. *Acta neuropathologica* **84**, 225-233, doi:10.1007/bf00227813 (1992).
81 Saman, S. *et al.* Exosome-associated tau is secreted in tauopathy models and is selectively phosphorylated in cerebrospinal fluid in early Alzheimer disease. *The Journal of biological chemistry* **287**, 3842-3849, doi:10.1074/jbc.M111.277061 (2012).
82 Simard, A. R., Soulet, D., Gowing, G., Julien, J. P. & Rivest, S. Bone marrow-derived microglia play a critical role in restricting senile plaque formation in Alzheimer's disease. *Neuron* **49**, 489-502, doi:10.1016/j.neuron.2006.01.022 (2006).
83 Santello, M., Cali, C. & Bezzi, P. Gliotransmission and the tripartite synapse. *Advances in experimental medicine and biology* **970**, 307-331, doi:10.1007/978-3-7091-0932-8_14 (2012).
84 González-Reyes, R. E., Nava-Mesa, M. O., Vargas-Sánchez, K., Ariza-Salamanca, D. & Mora-Muñoz, L. Involvement of Astrocytes in Alzheimer's Disease from a Neuroinflammatory and Oxidative Stress Perspective. *Frontiers in molecular neuroscience* **10**, 427, doi:10.3389/fnmol.2017.00427 (2017).
85 Brown, A. M. & Ransom, B. R. Astrocyte glycogen and brain energy metabolism. *Glia* **55**, 1263-1271, doi:10.1002/glia.20557 (2007).
86 Perea, G., Navarrete, M. & Araque, A. Tripartite synapses: astrocytes process and control synaptic information. *Trends in neurosciences* **32**, 421-431, doi:10.1016/j.tins.2009.05.001 (2009).
87 Kim, Y., Park, J. & Choi, Y. K. The Role of Astrocytes in the Central Nervous System Focused on BK Channel and Heme Oxygenase Metabolites: A Review. *Antioxidants (Basel)* **8**, 121, doi:10.3390/antiox8050121 (2019).
88 Sama, M. A. *et al.* Interleukin-1beta-dependent signaling between astrocytes and neurons depends critically on astrocytic calcineurin/NFAT activity. *The Journal of biological chemistry* **283**, 21953-21964, doi:10.1074/jbc.M800148200 (2008).
89 Liddelow, S. A. *et al.* Neurotoxic reactive astrocytes are induced by activated microglia. *Nature* **541**, 481-487, doi:10.1038/nature21029 (2017).
90 Kamphuis, W. *et al.* Glial fibrillary acidic protein isoform expression in plaque related astrogliosis in Alzheimer's disease. *Neurobiology of aging* **35**, 492-510, doi:10.1016/j.neurobiolaging.2013.09.035 (2014).
91 Gao, M. *et al.* Induced neural stem cell-derived astrocytes modulate complement activation and mediate neuroprotection following closed head injury. *Cell Death & Disease* **9**, 101, doi:10.1038/s41419-017-0172-7 (2018).
92 Moynagh, P. N. The interleukin-1 signalling pathway in astrocytes: a key contributor to inflammation in the brain. *J Anat* **207**, 265-269, doi:10.1111/j.1469-7580.2005.00445.x (2005).
93 Sollvander, S. *et al.* Accumulation of amyloid-beta by astrocytes result in enlarged endosomes and microvesicle-induced apoptosis of neurons. *Mol Neurodegener* **11**, 38, doi:10.1186/s13024-016-0098-z (2016).
94 Butterfield, D. A., Swomley, A. M. & Sultana, R. Amyloid β-peptide (1-42)-induced oxidative stress in Alzheimer disease: importance in disease pathogenesis and progression. *Antioxidants & redox signaling* **19**, 823-835, doi:10.1089/ars.2012.5027 (2013).

95 Jo, S. *et al.* GABA from reactive astrocytes impairs memory in mouse models of Alzheimer's disease. *Nat Med* **20**, 886-896, doi:10.1038/nm.3639 (2014).
96 Ma, Y. *et al.* Research progress of the relationship between pyroptosis and disease. *Am J Transl Res* **10**, 2213-2219 (2018).
97 Fink, S. L. & Cookson, B. T. Apoptosis, pyroptosis, and necrosis: mechanistic description of dead and dying eukaryotic cells. *Infection and immunity* **73**, 1907-1916, doi:10.1128/iai.73.4.1907-1916.2005 (2005).
98 Man, S. M., Karki, R. & Kanneganti, T. D. Molecular mechanisms and functions of pyroptosis, inflammatory caspases and inflammasomes in infectious diseases. *Immunological reviews* **277**, 61-75, doi:10.1111/imr.12534 (2017).
99 Wang, S., Yuan, Y. H., Chen, N. H. & Wang, H. B. The mechanisms of NLRP3 inflammasome/pyroptosis activation and their role in Parkinson's disease. *International immunopharmacology* **67**, 458-464, doi:10.1016/j.intimp.2018.12.019 (2019).
100 Liu, X. *et al.* Inflammasome-activated gasdermin D causes pyroptosis by forming membrane pores. *Nature* **535**, 153-158, doi:10.1038/nature18629 (2016).
101 Shi, J. *et al.* Cleavage of GSDMD by inflammatory caspases determines pyroptotic cell death. *Nature* **526**, 660-665, doi:10.1038/nature15514 (2015).
102 Sborgi, L. *et al.* GSDMD membrane pore formation constitutes the mechanism of pyroptotic cell death. *The EMBO journal* **35**, 1766-1778, doi:10.15252/embj.201694696 (2016).
103 Jerónimo-Santos, A. *et al.* Dysregulation of TrkB Receptors and BDNF Function by Amyloid-β Peptide is Mediated by Calpain. *Cerebral cortex (New York, N.Y. : 1991)* **25**, 3107-3121, doi:10.1093/cercor/bhu105 (2015).
104 Kemppainen, S. *et al.* Impaired TrkB receptor signaling contributes to memory impairment in APP/PS1 mice. *Neurobiology of aging* **33**, 1122.e1123-1139, doi:10.1016/j.neurobiolaging.2011.11.006 (2012).
105 Belo, R. F. *et al.* The Neuroprotective Action of Amidated-Kyotorphin on Amyloid β Peptide-Induced Alzheimer's Disease Pathophysiology. *Front Pharmacol* **11**, 985, doi:10.3389/fphar.2020.00985 (2020).
106 Hoffmann, A. C. *et al.* Extracellular aggregated alpha synuclein primarily triggers lysosomal dysfunction in neural cells prevented by trehalose. *Scientific reports* **9**, 544, doi:10.1038/s41598-018-35811-8 (2019).
107 Giuffrida, M. L. *et al.* Beta-amyloid monomers are neuroprotective. *The Journal of neuroscience : the official journal of the Society for Neuroscience* **29**, 10582-10587, doi:10.1523/jneurosci.1736-09.2009 (2009).
108 Buskila, Y. *et al.* Extending the viability of acute brain slices. *Scientific reports* **4**, 5309, doi:10.1038/srep05309 (2014).
109 Aydin, S. A short history, principles, and types of ELISA, and our laboratory experience with peptide/protein analyses using ELISA. *Peptides* **72**, 4-15, doi:10.1016/j.peptides.2015.04.012 (2015).
110 Kummitha, C. M. *et al.* A sandwich ELISA for the detection of Wnt5a. *J Immunol Methods* **352**, 38-44, doi:10.1016/j.jim.2009.11.005 (2010).
111 Indalao, I. L., Sawabuchi, T., Takahashi, E. & Kido, H. Correction to: IL-1b is a key cytokine that induces trypsin upregulation in the influenza virus-cytokine-trypsin cycle. *Arch Virol* **163**, 3487-3487, doi:10.1007/s00705-018-4043-z (2018).
112 Towbin, H., Staehelin, T. & Gordon, J. Electrophoretic transfer of proteins from polyacrylamide gels to nitrocellulose sheets: procedure and some applications. *Proceedings of the National Academy of Sciences* **76**, 4350, doi:10.1073/pnas.76.9.4350 (1979).
113 Mahmood, T. & Yang, P.-C. Western blot: technique, theory, and trouble shooting. *N Am J Med Sci* **4**, 429-434, doi:10.4103/1947-2714.100998 (2012).

114 Hnasko, T. S. & Hnasko, R. M. The Western Blot. *Methods in molecular biology* **1318**, 87-96, doi:10.1007/978-1-4939-2742-5_9 (2015).
115 Yang, Z. & Wang, K. K. W. Glial fibrillary acidic protein: from intermediate filament assembly and gliosis to neurobiomarker. *Trends in neurosciences* **38**, 364-374, doi:10.1016/j.tins.2015.04.003 (2015).
116 Ohsawa, K., Imai, Y., Sasaki, Y. & Kohsaka, S. Microglia/macrophage-specific protein Iba1 binds to fimbrin and enhances its actin-bundling activity. *J Neurochem* **88**, 844-856, doi:10.1046/j.1471-4159.2003.02213.x (2004).
117 Hopperton, K. E., Mohammad, D., Trépanier, M. O., Giuliano, V. & Bazinet, R. P. Markers of microglia in post-mortem brain samples from patients with Alzheimer's disease: a systematic review. *Molecular Psychiatry* **23**, 177-198, doi:10.1038/mp.2017.246 (2018).
118 Zhao, X. *et al.* Noninflammatory Changes of Microglia Are Sufficient to Cause Epilepsy. *Cell reports* **22**, 2080-2093, doi:10.1016/j.celrep.2018.02.004 (2018).
119 Kosmidou, C. *et al.* Issues with the Specificity of Immunological Reagents for NLRP3: Implications for Age-related Macular Degeneration. *Scientific reports* **8**, 461-461, doi:10.1038/s41598-017-17634-1 (2018).
120 Swanson, K. V., Deng, M. & Ting, J. P. Y. The NLRP3 inflammasome: molecular activation and regulation to therapeutics. *Nature Reviews Immunology* **19**, 477-489, doi:10.1038/s41577-019-0165-0 (2019).
121 Nakanishi, A. *et al.* Amyloid β directly interacts with NLRP3 to initiate inflammasome activation: identification of an intrinsic NLRP3 ligand in a cell-free system. *Inflammation and Regeneration* **38**, 27, doi:10.1186/s41232-018-0085-6 (2018).
122 Savage, C. D., Lopez-Castejon, G., Denes, A. & Brough, D. NLRP3-Inflammasome Activating DAMPs Stimulate an Inflammatory Response in Glia in the Absence of Priming Which Contributes to Brain Inflammation after Injury. *Frontiers in immunology* **3**, 288-288, doi:10.3389/fimmu.2012.00288 (2012).
123 Duraiyan, J., Govindarajan, R., Kaliyappan, K. & Palanisamy, M. Applications of immunohistochemistry. *J Pharm Bioallied Sci* **4**, S307-S309, doi:10.4103/0975-7406.100281 (2012).
124 Sherriff, F. E., Bridges, L. R. & Sivaloganathan, S. Early detection of axonal injury after human head trauma using immunocytochemistry for beta-amyloid precursor protein. *Acta neuropathologica* **87**, 55-62, doi:10.1007/bf00386254 (1994).
125 Matos, L. L., Trufelli, D. C., de Matos, M. G. & da Silva Pinhal, M. A. Immunohistochemistry as an important tool in biomarkers detection and clinical practice. *Biomarker insights* **5**, 9-20, doi:10.4137/bmi.s2185 (2010).
126 Wang, W.-Y., Meng, L.-J., Xu, Y.-J., Gong, T. & Yang, Y. Effects of 4% paraformaldehyde and modified Davidson's fluid on the morphology and immunohistochemistry of Xiang pig testes. *J Toxicol Pathol* **33**, 97-104, doi:10.1293/tox.2019-0072 (2020).
127 Sinha, N. *et al.* Comparitive efficacies of a natural fixative with a conventional fixative. *J Oral Maxillofac Pathol* **21**, 458-458, doi:10.4103/jomfp.JOMFP_236_15 (2017).
128 Drummond, E. & Wisniewski, T. Alzheimer's disease: experimental models and reality. *Acta neuropathologica* **133**, 155-175, doi:10.1007/s00401-016-1662-x (2017).
129 Liao, Y. F., Wang, B. J., Cheng, H. T., Kuo, L. H. & Wolfe, M. S. Tumor necrosis factor-alpha, interleukin-1beta, and interferon-gamma stimulate gamma-secretase-mediated cleavage of amyloid precursor protein through a JNK-dependent MAPK pathway. *The Journal of biological chemistry* **279**, 49523-49532, doi:10.1074/jbc.M402034200 (2004).
130 Coll, R. C. *et al.* MCC950 directly targets the NLRP3 ATP-hydrolysis motif for inflammasome inhibition. *Nature chemical biology* **15**, 556-559, doi:10.1038/s41589-019-0277-7 (2019).
131 Sun, D., Kintner, D. B. & Pond, B. B. in *Physiology and Pathology of Chloride Transporters and Channels in the Nervous System* (eds F. Javier Alvarez-Leefmans & Eric Delpire) 501-517 (Academic Press, 2010).

132 Brown, T. H. *et al.* in *From Molecules to Networks* (eds John H. Byrne & James L. Roberts) 499-574 (Academic Press, 2004).
133 Yun, S. P. *et al.* Block of A1 astrocyte conversion by microglia is neuroprotective in models of Parkinson's disease. *Nat Med* **24**, 931-938, doi:10.1038/s41591-018-0051-5 (2018).
134 Pekny, M., Wilhelmsson, U. & Pekna, M. The dual role of astrocyte activation and reactive gliosis. *Neuroscience letters* **565**, 30-38, doi:https://doi.org/10.1016/j.neulet.2013.12.071 (2014).
135 Hou, B. *et al.* Inhibition of the NLRP3-inflammasome prevents cognitive deficits in experimental autoimmune encephalomyelitis mice via the alteration of astrocyte phenotype. *Cell Death Dis* **11**, 377, doi:10.1038/s41419-020-2565-2 (2020).
136 Lian, H. *et al.* NFκB-activated astroglial release of complement C3 compromises neuronal morphology and function associated with Alzheimer's disease. *Neuron* **85**, 101-115, doi:10.1016/j.neuron.2014.11.018 (2015).
137 Zotova, E. *et al.* Inflammatory components in human Alzheimer's disease and after active amyloid-β42 immunization. *Brain : a journal of neurology* **136**, 2677-2696, doi:10.1093/brain/awt210 (2013).
138 Martinez, F. O. *et al.* Genetic programs expressed in resting and IL-4 alternatively activated mouse and human macrophages: similarities and differences. *Blood* **121**, e57-69, doi:10.1182/blood-2012-06-436212 (2013).
139 Trombetta, A. C. *et al.* A circulating cell population showing both M1 and M2 monocyte/macrophage surface markers characterizes systemic sclerosis patients with lung involvement. *Respiratory Research* **19**, 186, doi:10.1186/s12931-018-0891-z (2018).
140 Bertani, F. R. *et al.* Classification of M1/M2-polarized human macrophages by label-free hyperspectral reflectance confocal microscopy and multivariate analysis. *Scientific reports* **7**, 8965-8965, doi:10.1038/s41598-017-08121-8 (2017).
141 Rőszer, T. Understanding the Mysterious M2 Macrophage through Activation Markers and Effector Mechanisms. *Mediators of Inflammation* **2015**, 816460, doi:10.1155/2015/816460 (2015).
142 Frank, M. G., Weber, M. D., Watkins, L. R. & Maier, S. F. Stress-induced neuroinflammatory priming: A liability factor in the etiology of psychiatric disorders. *Neurobiology of Stress* **4**, 62-70, doi:https://doi.org/10.1016/j.ynstr.2015.12.004 (2016).
143 Luo, B. *et al.* NLRP3 Inflammasome as a Molecular Marker in Diabetic Cardiomyopathy. **8**, doi:10.3389/fphys.2017.00519 (2017).
144 Gaidt, M. M. & Hornung, V. Pore formation by GSDMD is the effector mechanism of pyroptosis. *The EMBO journal* **35**, 2167-2169, doi:10.15252/embj.201695415 (2016).
145 Haas, M. *et al.* The European Medicines Agency's strategies to meet the challenges of Alzheimer disease. *Nature reviews. Drug discovery* **14**, 221-222, doi:10.1038/nrd4585 (2015).
146 Sidiqi, A. M. *et al.* In vivo imaging of curcumin labeled amyloid beta deposits in retina using fluorescence scanning laser ophthalmoscopy in an Alzheimer mouse model. *Investigative Ophthalmology & Visual Science* **59**, 6065-6065 (2018).